https://doi.org/10.5194/egusphere-2026-4723
Preprint. Discussion started: 18 August 2026

Enhanced ocean mixing improves proxy-model agreement for an Early Pliocene seasonally ice-free Arctic Ocean

Jochen Knies[1,2], Christian Stepanek[3], Simon T. Belt[4], Stijn De Schepper[5,6], and Gerrit Lohmann[3,7]

[1] iC3 – Centre for ice, Cryosphere, Carbon and Climate, Department of Geosciences, UiT The Arctic University of Norway, 9037 Tromsø, Norway
[2] Geological Survey of Norway, 7491 Trondheim, Norway
[3] Alfred Wegener Institute Helmholtz Centre for Polar and Marine Research, Bremerhaven, Germany
[4] SBelt$_{25}$ Consulting, Ivybridge, Devon, PL21 0PN, UK
[5] NORCE Climate and Environment, Jahnebakken 5, 5008 Bergen, Norway
[6] University of Bergen, Department of Earth Science, Bjerknes Centre for Climate Research, Jahnebakken 5, 5008 Bergen, Norway
[7] University of Bremen, Physics Department and MARUM, 28334 Bremen, Germany

Correspondence to: Jochen Knies (jochen.knies@uit.no)

Summary. The Arctic is rapidly approaching seasonally ice-free ("blue") conditions. Using proxy data to evaluate simulations of past warm climates, we show that enhanced ocean mixing substantially improves agreement with evidence for a blue Arctic and reveals multiple pathways for Arctic warming during the Early Pliocene. Our findings highlight the importance of accurately representing ocean processes in climate models to improve projections of future Arctic climate.

https://doi.org/10.5194/egusphere-2026-4723
Preprint. Discussion started: 18 August 2026

Abstract. The Arctic Ocean rapidly transitions towards ice-free summers, a **"**blue**"** (i.e., summer sea ice-free) state driven by Arctic amplification of abrupt global warming. To improve climate projections and better understand the consequences of reduced Arctic sea ice in a warming climate, it is essential to examine past warm intervals such as the Early Pliocene (~5–4 Ma), when diminished Arctic sea ice coincided with higher global temperatures. Proxy records from the Arctic-Atlantic Gateway (AAG) (~70–80°N), combined with climate model simulations, indicate periodically ice-free summers during this time. Yet, model-data comparisons for the central Arctic Ocean (>80°N) reveal winter sea ice as a persistent feature. Here, we show that proxy evidence for a "blue" Arctic is best reproduced when enhanced vertical ocean mixing is integrated into climate models. Under enhanced mixing, Arctic warming occurs through different mechanisms depending on the model geography, whereas simulations with standard mixing show substantially weaker agreement with proxy evidence. We do not interpret enhanced mixing as the unique solution but rather as a physically motivated sensitivity test that represents unresolved ocean processes. Our results demonstrate that modifying a single ocean parameterization within physically plausible boundaries substantially improves proxy-model agreement for a warmer than modern Early Pliocene, both at the AAG and for the wider Arctic. Combined with published proxy evidence for a warmer Arctic Ocean interior, our findings underscore the need for improved representation of ocean dynamics in paleoclimate simulations. Next-generation climate models should evaluate the sensitivity of simulated "blue" Arctic climates to ocean mixing alongside other key processes, including cloud microphysics and radiative feedbacks, to increase confidence in projections of seasonally ice-free Arctic conditions.

https://doi.org/10.5194/egusphere-2026-4723
Preprint. Discussion started: 18 August 2026

1 Introduction

There is overwhelming agreement that the Arctic Ocean and its surroundings are subject to rapid and dramatic environmental changes today and over the course of historical and geological time-scales (Slater et al., 2021; Moran et al., 2006; Stein, 2019). Owing to complex feedback processes that substantially increase a global warming signal within the polar regions, a phenomenon collectively known as "polar amplification", the Arctic is both a contributor to ongoing climate change and among those regions that will be most affected by global warming. Among the implicated changes are massive reduction in Arctic sea ice coverage and melting of glacial ice on Greenland, which are approaching threshold conditions beyond which rapid global changes are likely (Pörtner et al., 2019). One of the most dramatic trends observed in the Arctic Ocean during the recent past is the rapid reduction in Arctic sea ice extent (Kinnard et al., 2011), with projections suggesting a practically ice-free Arctic in summer months by the 2050s (Notz and Stroeve, 2016; Kim et al., 2023; Jahn et al., 2024). Although coupled atmosphere-ocean-ice model simulations suggest that the recent warming in the Northern Hemisphere is responsible for this decline (Notz and Stroeve, 2016), there is disagreement between proxy data and models regarding the impact of atmospheric warming versus oceanic heat transport on sea ice decline and glacial mass loss, with appreciable model-dependency (Slater et al., 2021; Selivanova et al., 2024; Docquier et al., 2019), highlighting parameterized processes – and the parameter values used to represent them – as a source of potential uncertainty in climate models.

As we enter uncharted territory in a rapidly warming Arctic as a result of anthropogenic climate change, it is important to address the impact of parameter uncertainty in climate models, whose settings are tuned to the modern observational period as a benchmark, and which may therefore not generalize to substantially different climate states. Parameter uncertainty is one part of modelling uncertainty as described in the Paleoclimate Modelling Intercomparison Project

https://doi.org/10.5194/egusphere-2026-4723
Preprint. Discussion started: 18 August 2026

(PMIP) triangle of model-data discrepancy (Haywood et al., 2016). This uncertainty may become relevant when applying climate models to past warm climates, where model parameters provide one source of model spread in simulating a "blue" (i.e., summer sea ice-free) Arctic. Past warm climates therefore serve as an independent test for the assumption of parameter robustness across timescales.

In order to improve our understanding of Arctic sea ice variability and continental ice reduction, particularly in the context of current rapid global warming, and to improve the reliability of climate model projections of a future Arctic, improvements to proxy- and model-based sea ice, sea surface temperature (SST) and surface air temperature (SAT) reconstructions from past, globally warmer climates (Fig. 1) are thus imperative to quantify model-data mismatch as a first step of addressing sources of modelling uncertainty.

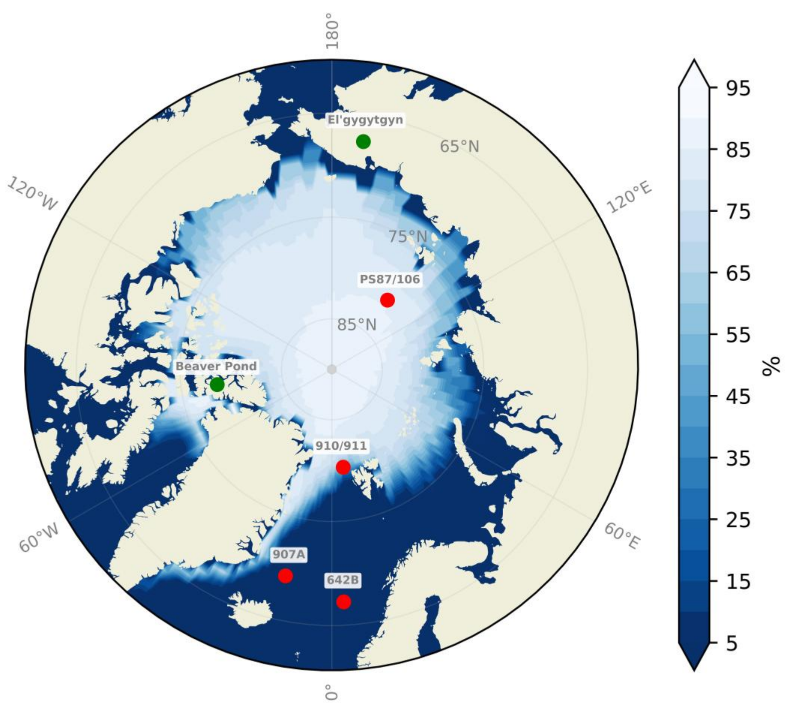

Figure 1: Site locations of past Arctic warmth and modelled present-day sea ice. Simulated multiyear annual minimum (i.e., September) Arctic sea ice concentration (percentage of grid cell area; blue to white shading) for a pre-industrial reference state. Marine site locations of Ocean Drilling Program (ODP) Site 910 (80.2649°N, 6.5901°E), Site 907 (69.2498°N, -12.6982°W), Site 642 (67.225°N, 02.9283°E), as well as central Arctic Ocean sediment core PS87/106-1 (81.21267°N, 141.1745°E) are indicated by red circles. Terrestrial sites from Canada's High Arctic (Ellesmere Island, Beaver Pond locality at 78.55°N, 82.4167°W) and Siberian Arctic (Lake El'gygytgyn at 67.5°N, 172°E) are indicated by green circles. Modern land sea mask from observational data indicated via yellowish brown shading.

The Pliocene epoch (5.33–2.58 million years ago (Ma)) featured a dynamic climate with pronounced glacial-interglacial cycles, and parts of the Pliocene climate were characterized by environmental conditions comparable to climate projections for the coming decades to centuries (Burke et al., 2018; Oldeman et al., 2024; De Nooijer et al., 2020; Mcclymont et al., 2023), with atmospheric carbon dioxide (CO_2) concentrations (~400-500 ppm from the Miocene into the Pliocene (Sosdian et al., 2018)) comparable to those predicted for the future (Steinthorsdottir et al., 2021; Berends et al., 2019; Burls et al., 2021b; Herold et al., 2012; Zhang et al., 2013; Super et al., 2018; Martínez-Botí et al., 2015; Stap et al., 2016), particularly for the Early Pliocene (Zanclean, ~5.3-3.6 Ma) (Ballantyne et al., 2010; Csank et al., 2011c; Ballantyne et al., 2013; Knies et al., 2014a; Clotten et al., 2019; De Schepper et al., 2014; Tedford and Harington, 2003). Despite its relevance, the Arctic Ocean remains, paradoxically, geologically underexplored in terms of past "warmer-than-present" climate states. Compounding this knowledge gap, the continental configuration, mountain topography, and global ocean circulation during the Early Pliocene were different from modern conditions (Steinthorsdottir et al., 2021; Knies et al., 2014b), which complicates the interpretation of proxy-based reconstructed climate patterns – a problem that can be mitigated by utilising numeric climate models capable of providing

https://doi.org/10.5194/egusphere-2026-4723
Preprint. Discussion started: 18 August 2026

physically-based representations of past warm climates, while taking into account impacts of differences of forcings and paleogeography relative to today.

Here, we test the hypothesis that the Arctic Ocean was "blue" (i.e., summer sea ice-free) during the Early Pliocene. On the climate modelling side we employ COSMOS, a model whose sensitivity to different characteristics of Pliocene and Miocene climate drivers has been explored in detail. The geographic reconstructions leveraged by us have been widely employed within the Pliocene Model Intercomparison Project (PlioMIP) via the mid-Piacenzian Warm Period configuration (PRISM4; Dowsett et al., 2016) with 400 ppmv of carbon dioxide (simulation Eoi400; Haywood et al., 2016). Due to the absence of dedicated COSMOS Early Pliocene simulations within the PlioMIP2 (Haywood et al., 2016) and Miocene Model Intercomparison Project (MioMIP) frameworks (Burls et al., 2021a) that provide the foundation for the study presented here, we explore Early Pliocene climate conditions by evaluating climate patterns of both Late Pliocene and Miocene climate simulations prepared with the COSMOS. We acknowledge that previous work exists regarding modelling the climate of the Early Pliocene (Ford et al., 2022), but with a focus on the North Pacific rather than the geographic region we address in this manuscript. The Early Pliocene differs notably from the Late Pliocene simulations of PlioMIP2, particularly in terms of higher atmospheric CO_2 concentrations and relatively limited changes in paleogeography (e.g., a potentially open Central American Seaway (CAS) (Haywood et al., 2024)). To better capture the impact of these conditions in the research presented here we supplement our analysis of available Pliocene simulations with Miocene simulations that incorporate these key characteristics. In the framework of this study, Miocene simulations are not interpreted as direct reconstructions of the Early Pliocene but as warm-climate end-member experiments that help constrain the sensitivity of Arctic climate to gateway geometry and background warmth. Consideration of this aspect highlights the role of a potentially open CAS during the Early Pliocene for controlling details of processes that cause Arctic warmth.

https://doi.org/10.5194/egusphere-2026-4723
Preprint. Discussion started: 18 August 2026

To further investigate the influence of Arctic warmth on regional sea ice, we explore a range of atmospheric CO_2 concentrations and levels of vertical ocean mixing. In this study, enhanced vertical mixing serves as a surrogate for unresolved ocean processes that could have amplified high-latitude warming if fully represented in the model, such as stronger ocean mixing associated with different tidal dissipation under past sea-level configurations. It also provides a means to assess the limited sensitivity of climate models to prescribed paleogeography and greenhouse gas forcing. Our choice to employ two model setups for the mid-Piacenzian (mPLIO) and middle Miocene (MIO) that not only consider modern intensity of vertical mixing in the ocean (as in simulation PI (pre-industrial), but also enhanced background mixing in the ocean, is informed by the inference that vertical mixing parameters are weakly constrained, and that their calibration for a modern climate does not necessarily hold for other climates.

Our comparison of reconstructed and simulated climate patterns indicates that the modeled climate better matches Early Pliocene proxy data in the AAG when using Late Pliocene (mPLIO) and Miocene (MIO) boundary conditions – our available model analogue for the Early Pliocene – combined with enhanced vertical ocean mixing, with comparable improvements in model-data agreement also seen across the wider Arctic. This increased mixing warms the deep ocean and boosts meridional heat transport, thereby reducing meridional temperature gradients and amplifying Arctic warmth in combination with a cascade of feedbacks that impacts surface energy balance and lead to further warmth, from reduced surface albedo and increased evaporative coupling of atmosphere and ocean, via water vapor feedback to lapse rate feedback. Consequently, while the pre-industrial (PI) reference simulation maintains near freezing SST, extensive sea ice cover, and substantial ice thickness, our Pliocene and Miocene simulations show significantly reduced or absent sea ice in the AAG region, with comparable warming-driven improvements of model bias with respect to reconstructions found across the Arctic. Notably, however, even with enhanced mixing, all simulations presented here show that the broader Arctic Ocean remains ice-covered during winter months – indicating that the “blue” Arctic during the

Early Pliocene was a pattern focused on the summer season rather than a year-round phenomenon.

2 The Early Pliocene in the Arctic Ocean

During the Early Pliocene, when global CO_2 reached ~470 ppm (Martínez-Botí et al., 2015; Stap et al., 2016), tectonic boundary conditions in the Arctic Ocean were different from those of today, with small and shallow conduits between the Arctic Ocean and the World Ocean, except for the deep AAG (i.e., the Fram Strait). The Bering Strait possibly opened at the Miocene–Pliocene transition, around 5.5–5.3 Ma (Hall et al., 2023; Gladenkov et al., 2002), with flooding facilitated by large-scale tectonic events and/or eustatic sea-level rise (Marincovich Jr, 2000). The Barents Sea shelf was subaerially exposed in the Early Pliocene (Knies et al., 2014b), with major parts probably subsiding below sea level not before the middle Pleistocene (~0.7 Ma) (Patton et al., 2024). Shallow conduits through the Canadian Arctic Archipelago might not yet have existed in the Early Pliocene (Matthiessen et al., 2009), and the Bering and Fram Straits might have been the only gateways to the Arctic Ocean, with eustatic sea level varying on average by ±20 m around the modern level (Miller et al., 2011). A synthesis of Early Pliocene global environments (Salzmann et al., 2011) shows a northwards shift of temperate and boreal vegetation zones in the Pliocene in response to a warmer and wetter climate. Similar findings for the later part of the Pliocene have been derived from a reconstruction of mid-Piacenzian geography (Salzmann et al., 2013), and the importance of vegetation changes during the mid-Pliocene has been highlighted (Haywood et al., 2013). Simulations in PlioMIP2 have shown that this flattening of present-day climatic gradients permitted the expansion of evergreen forest to the shore of the Arctic Ocean (Stepanek et al., 2020) and provided wider geographic ranges for Asian mammalian communities (Tedford and Harington, 2003; Rybczynski et al., 2013). Relatively small-scale glaciations during the Early Pliocene were succeeded by a progressive intensification of glaciation in the latest

https://doi.org/10.5194/egusphere-2026-4723
Preprint. Discussion started: 18 August 2026

Pliocene (Jansen et al., 2000; Kleiven et al., 2002; Knies et al., 2014a; De Schepper and Mcclymont, 2025).

Evolution of central Arctic Ocean paleoceanography during the Early Pliocene is inferred from records in cores recovered by the Ocean Drilling Program (ODP) at the marginal Arctic Ocean and Nordic Seas. A compilation of data available from previous work (Fig. 2) shows that the few available reconstructions of Early Pliocene sea ice and SST indicate warm temperatures consistent with at least seasonally ice-free summer conditions prior to 4-4.5 Ma (Brigham-Grette and Carter, 1992; Cronin et al., 1993; Robinson, 2009; Knies et al., 2014a; Clotten et al., 2019). More specifically, absence of the highly branched isoprenoid (HBI) IP_{25}, a source-specific biomarker for seasonal Arctic sea ice due to its production by certain Arctic sympagic (sea ice-associated) diatoms (Belt et al., 2013; Brown et al., 2014), and distributions of glycerol dialkyl glycerol tetraethers (GDGTs) and hydroxylated GDGTs, demonstrate ice-free conditions during summers, with summer SST ranging from ~5–10°C between ~5.3 and ~4.0 Ma in the marginal Arctic Ocean (ODP Site 910) (Knies et al., 2014a) (Fig. 2). However, we note that in nearby ODP Site 911, two out of three studied samples between 5.0 and 4.0 Ma show the presence of IP_{25}, suggesting some seasonal sea ice in the study area (Clotten et al., 2019). In the western Nordic Seas (ODP Site 907, Iceland Sea) IP_{25} - inferred sea ice coverage appeared as early as ~4.5 Ma (Clotten et al., 2019) with alkenone-based SSTs ranges between ~8 and 13°C from ~5.3 to 4.5 Ma (Herbert et al., 2016) (Fig. 2). In the eastern Nordic Seas (ODP Site 642, Vøring Plateau) alkenone-based SST reconstruction ranges between ~11 and 16°C from ~5.3 to 4.2 Ma (Bachem et al., 2017). Further, the relatively high SSTs at ODP Sites 910 and 907 are consistent with warm summer periods recorded in Alaska (Reinink-Smith and Leopold, 2005) and Ellesmere Island, Arctic Canada (Csank et al., 2011c; Tedford and Harington, 2003).

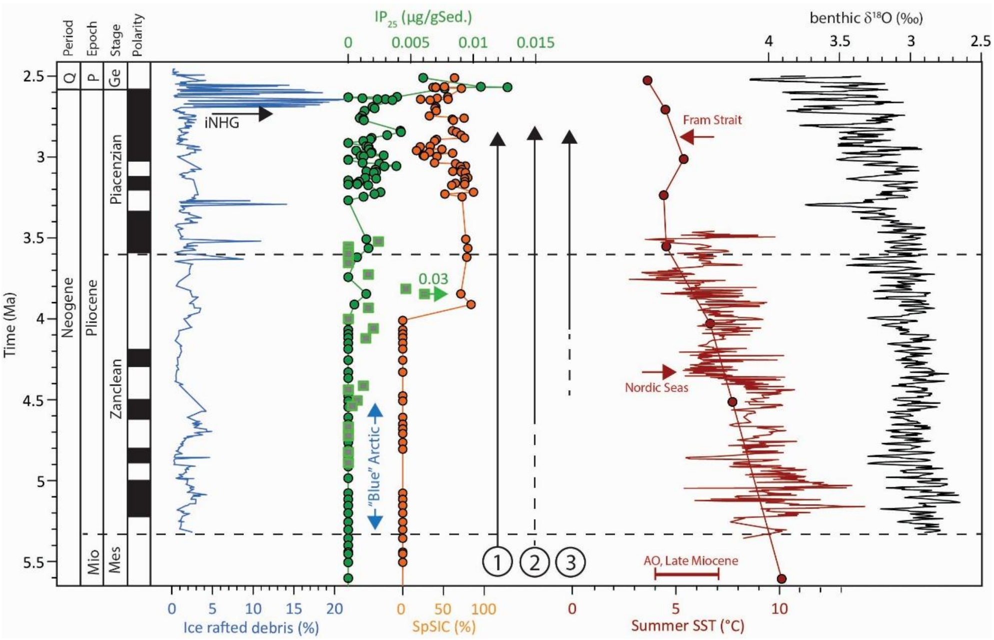

Figure 2. Climate proxy observations in the Arctic-Atlantic gateway (AAG) during the Pliocene epoch. Ice-rafted debris (IRD; wt.%, coarse fraction 100–1000 µm) recorded in ODP Site 911 (Knies et al., 2014a). Concentration of highly branched isoprenoid IP_{25} (in µg/g Sed.) in ODP Site 910 (circles) and Site 907 (squares) (Knies et al., 2014a; Clotten et al., 2019). Spring sea ice concentration (SpSIC in %) for ODP Site 910 (Rahaman et al., 2020) was calculated using a regional biomarker-based calibration (Smik et al., 2016). Sea surface temperatures (SST, in ºC) derived from glycerol dialkyl glycerol tetraethers (GDGTs) in ODP Site 910 and long-chain alkenones in ODP 907 (Knies et al., 2014a; Herbert et al., 2016) and global benthic $\delta^{18}O$ LR04-stack (Lisiecki and Raymo, 2005). SST derived from long-chain alkenones in Arctic Ocean (AO) is indicated for the Late Miocene (PS87/106-1) (Stein et al., 2016). Major key tectonic and palaeoenvironmental events are indicated by vertical continuous (certain) and stippled (uncertain) arrows: 1. Sub-aerial exposure of the Barents Sea (Patton et al., 2024). 2. Northward throughflow of Pacific waters into the Arctic Ocean through the Bering Strait (Hall et al., 2023). 3. Modern East Greenland Current (Clotten et al., 2019). INHG: Intensification of Northern Hemisphere Glaciation. "Winter sea ice": Modern (pre-industrial) winter sea ice extent in the Arctic Ocean established at ~2.6 million years ago (Knies et al.,

https://doi.org/10.5194/egusphere-2026-4723
Preprint. Discussion started: 18 August 2026

2014a). "Blue Arctic": Interval during the Early Pliocene with summer ice-free conditions in the Arctic Ocean.

During the Early Pliocene, the latter hosted modern-type boreal forests that are located at latitudes ~15 to 20° further south in modern times, and summer temperatures were 10 °C higher than today (Csank et al., 2011c; Ballantyne et al., 2010; Rybczynski et al., 2013). These findings are consistent with reported alkenone-based SST estimates of ~4–7 °C from the Late Miocene Arctic Ocean (Fig. 2) (Stein et al., 2016). These reconstructed proxy-based temperature estimates are also considerably warmer than those reproduced by several Late Pliocene model simulations at high latitudes (Haywood et al., 2024; Haywood et al., 2020; Haywood et al., 2013). Together, these findings support the notion that, during the Early Pliocene, between 4.5 and ~5.3 Ma, and extended into the Late Miocene, the Arctic Ocean experienced largely ice-free summers, with only the central part of the Arctic Ocean remaining ice-covered during winter months (Ballantyne et al., 2013; Stein et al., 2016).

3 Materials and methods

We explore the response of simulated Pliocene and Miocene climate to different ocean vertical mixing parameter settings. Our aim is to quantify the skill of our climate simulations to reproduce different aspects of the reconstructed paleoenvironment of the Early Pliocene, and across the wider Pliocene-Miocene framework. Our analysis will also trace the different pathways of excess heat reaching the Arctic in dependence of the background paleogeography implemented in our models. The methods employed to this end are outlined below.

https://doi.org/10.5194/egusphere-2026-4723
Preprint. Discussion started: 18 August 2026

3.1 Model description

The COmmunity earth System MOdelS (COSMOS) suite (Jungclaus et al., 2006) is a numeric- and algorithm-based quantitative representation of the state and dynamics of the coupled atmosphere-land surface-ocean-sea ice system and has been extensively applied to various climate states since the Cretaceous, across the Cenozoic, through the Quaternary, and into the future. In particular, the COSMOS has been applied in numerous Pliocene and Miocene climate modeling studies (Stepanek and Lohmann, 2012; Haywood et al., 2020; Haywood et al., 2013; Stepanek et al., 2020; Burls et al., 2021b; Hossain et al., 2021; Stärz et al., 2017) employing different model configurations with and without vegetation dynamics (Stepanek et al., 2020; Stepanek and Lohmann, 2012), and with different sets of ocean mixing parameterizations (Lohmann et al., 2022). The behavior of the COSMOS in response to external climate forcing across various background climates and paleogeographies is therefore well characterized, including its climate metrics such as polar amplification and climate sensitivity, and the role of vegetation dynamics and related feedbacks in a changing Arctic.

The COSMOS has been assembled from two major components – one for ocean and sea ice dynamics, and one for atmosphere and land surface dynamics. The ocean component MPIOM (Marsland et al., 2003) is a z-coordinate global general circulation model with free surface, employing Boussinesq and hydrostatic approximations at 40 unevenly-spaced vertical levels. It includes a viscous-plastic rheology Hibler-type sea-ice component. In our model setup the MPIOM is formulated on a bipolar curvilinear Arakawa-C grid of a formal horizontal resolution of ~1.8°x3.0° (longitude/latitude). Its characteristics include increased resolution in major deepwater formation regions of the North Atlantic-Arctic realm (Fig. 3) (Marsland et al., 2003), that enhances the realism of the simulation of physical processes in the North Atlantic and towards the Arctic. Its sea ice component considers the insulating effects of snow (Marsland et al., 2003).

https://doi.org/10.5194/egusphere-2026-4723
Preprint. Discussion started: 18 August 2026

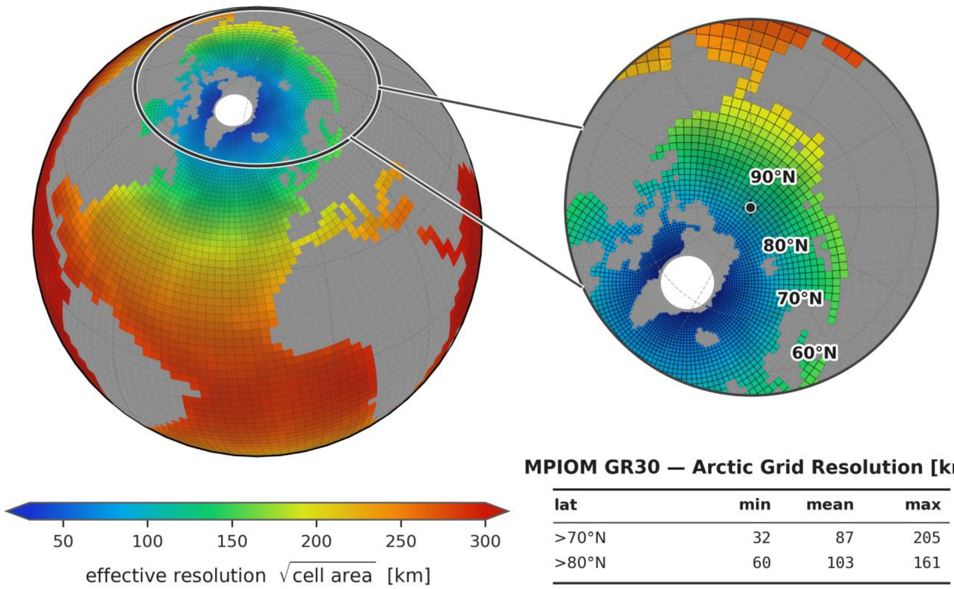

MPIOM GR30 — Arctic Grid Resolution [km]

lat	min	mean	max
>70°N	32	87	205
>80°N	60	103	161

Figure 3. Arctic refinement of horizontal resolution on the GR30 ocean grid employed in this study. Shown is the geometry for scalar ocean grid cells on which quantities presented in this study (temperature, sea ice) are present. Effective resolution (that is the square root of grid cell area, taking into account that grid cell borders are slightly curved) illustrated via color shades, grid cell borders indicated by thin lines, land indicated by grey shading. Statistics of grid geometries in specific latitude bands, presented in the table, are computed for ocean cells only. We show the case for a modern geography. While the grid itself is kept constant across simulations presented in this study, bathymetry and the land-sea distribution changes for Pliocene and Miocene simulations.

The atmosphere component ECHAM5 (Roeckner et al., 2003) is a global model of general circulation of the atmosphere with a spectral dynamical core. It is formulated on a vertical hybrid sigma-pressure coordinate and a horizontal Gaussian grid. For this study the model employs 19 vertical levels and a grid resolution of 3.75°x3.75°. It features a cloud microphysics scheme and the capability to simulate mixed-phase clouds (Roeckner et al., 2006) and includes a

https://doi.org/10.5194/egusphere-2026-4723
Preprint. Discussion started: 18 August 2026

representation of the atmospheric boundary layer (Roeckner et al., 2003) that is important for simulating the positive lapse rate feedback in the Arctic (Pithan and Mauritsen, 2014). In the fully coupled atmosphere-ocean setup the included hydrological discharge scheme (Hagemann and Gates, 2001; Hagemann and Dümenil, 1997) redirects excess precipitation along the orographic slope back to the ocean and closes the hydrological cycle between land and atmosphere. The internally coupled land surface component JSBACH (Raddatz et al., 2007) implements various land surface processes, among them dynamic vegetation, enabling the simulation of climate-vegetation feedbacks (Brovkin et al., 2009). Vegetation dynamics in the model are particularly useful for climate states that differ significantly from today, and for which no global vegetation distribution exists that is consistent with simulated climate conditions and that could be provided as a climate-consistent boundary condition (Stepanek et al., 2020). While both MioMIP and PlioMIP provide vegetation distributions as a climate model forcing, there is generally no adaptation of these fields provided for applications in climates with different degrees of warmth in the model due to, for example, modification of the employed CO_2 forcing, or, in the case of our study, use of enhanced ocean vertical mixing. In our simulations, consistency between climate and model vegetation is automatically achieved via vegetation dynamics, and presence of climate-vegetation dynamics is assured.

To enable ensembles of multi-millennial simulations to reach quasi-equilibrium for very different climate states, spatial resolution in the COSMOS is kept low. Various improvements of the representation of physical processes at coarse spatial resolution are considered by the COSMOS via dedicated parameterizations. On the ocean side, these include a formulation of isopycnal mixing following Redi (1982), a parameterization of tracer transport by unresolved mesoscale eddies via eddy-induced velocity (Gent et al., 1995), and a parameterization of vertical mixing and diffusion after Pacanowski and Philander (PP) (Pacanowski and Philander, 1981), which represents a common mixing scheme in paleoclimate research due to its straightforward incorporation and computational efficiency. Other mixing parameterization schemes exist, but all of them possess limitations that lead to uncertainty in climate simulations. Further improvements of the simulation of ocean dynamics address flow along ocean bottom structures via a slope-convection algorithm, and consideration of partial grid cells that improve the realism of prescribed ocean bathymetry. In the atmosphere, small-scale features of land surface orography are considered via a sub-gridscale parameterization of gravity wave drag.

3.2 Experimental design

While the Early Pliocene is less well sampled based on climate models, the Late Pliocene is quite well understood from the viewpoint of a multi-model perspective due to the mid-Piacenzian Warm Period having featured as the core time slice of the PlioMIP2. We take inferences from that modelling intercomparison as a foundation for discussing problems in model skill that we will then apply to the Early Pliocene. Generally, the magnitude of reconstructed North Atlantic temperature anomalies for the mid-Piacenzian is reproduced by only a small number of models (McClymont et al., 2020), with the majority being too cold (Dowsett et al., 2013; Salzmann et al., 2013). It is noteworthy that this tendency towards underestimation of Arctic warmth exists even though the PlioMIP2 mid-Piacenzian Warm Period continental configuration contains a closed Bering Strait. While this geographic feature warms the North Atlantic to Arctic region via enhanced ocean heat transport (Otto-Bliesner et al., 2017), the realism of a closed Bering Strait during the mid-Piacenzian still remains debated (Haywood et al., 2020; Hall et al., 2023). Within the context of the Pliocene, it has been furthermore shown that models fail to reproduce ice-free Arctic summers when Arctic feedbacks and polar amplification are suppressed (Salzmann et al., 2013).

These previous findings close our argumentative chain to study the impact of enhanced vertical mixing in the ocean on agreement between modelled and reconstructed climate patterns of the Pliocene to Miocene. Since no equivalent enhanced ocean mixing sensitivity simulations exist within the controlled PlioMIP2 ensemble (Haywood et al., 2016), we consider the COSMOS climate simulations presented here as being among the best available tests for our hypothesis that enhanced ocean vertical mixing may improve agreement between proxy evidence and models. Two lines of evidence suggest the COSMOS as a robust tool to further examine the impact of adapted ocean mixing parameters on the state of the Arctic and agreement between climate model and proxy-evidence. The COSMOS has a climate sensitivity of 4.7°C per doubling of carbon dioxide (Stepanek et al., 2020), well above the average of PlioMIP2 ensemble models (Haywood et al., 2020). Simulated Arctic and global mid-Piacenzian near surface air temperature anomaly of the COSMOS are close to the ensemble mean (Haywood et al., 2020; De Nooijer et al., 2020). This indicates that Pliocene Arctic warmth in the COSMOS is at least average, and not on the cooler side, compared to similar models under equivalent forcing and geography. Therefore, a model-data mismatch in the COSMOS can be taken as indicative of a widespread limitation of Arctic warmth across the PlioMIP2 ensemble in comparison to Pliocene proxy records, rather than to be considered as an issue with the COSMOS itself. As a second line of evidence, this study explicitly demonstrates that COSMOS reproduces the key characteristics of pre-industrial Arctic sea ice and sea surface temperatures in the context of the Coupled Model Intercomparison Project (CMIP) Phase 5 and Phase 6 model ensembles. These ensembles provide extensive evaluation data through simulations from numerous models, including more recent generations (Sect. 4.1). We use model geographies and climate forcings that have been prepared in the framework of the PlioMIP2 (Haywood et al., 2016) and MioMIP efforts (Burls et al., 2021b). The PlioMIP2 and MioMIP reference simulations, named here mPLIO400 and MIO450 (where the former has 400 ppm of CO_2 prescribed, and the latter 450 ppm), bracket the Early Pliocene and

https://doi.org/10.5194/egusphere-2026-4723
Preprint. Discussion started: 18 August 2026

provide an envelope of climate patterns around the period of interest, reflecting uncertainty in details of geographic boundary conditions and model forcings. The long tectonic history of the CAS closure (detailed in Section 4.1) is used as the main argument to test the "blue" Arctic hypothesis with the MIO (open CAS) and mPLIO (closed CAS) setups. This aspect of modified low-latitude gateway differences between the Miocene and the Pliocene thus addresses the link between Pliocene and Miocene simulations and provides quantification of a gateway impact (Haywood et al., 2024). The absence of a compatible and commonly accepted modeling protocol for an Early Pliocene time slice in PlioMIP2, which could serve as a direct counterpart to our proxy reconstructions (Fig. 2), necessitates such an indirect modeling approach. We note, however, that the upcoming PlioMIP3 considers an Early Pliocene time slice (Haywood et al., 2024), which differs from our mPLIO400 simulation by featuring increased concentrations of CO_2 (490 ppm) and the presence of a Central American Seaway (CAS). Once these simulations are produced and released to the community, an additional perspective on Early Pliocene climate will become available.

A key component of the simulation of processes in the ocean considered in this study is the ocean vertical mixing scheme of the COSMOS that simulates diapycnal mixing via two parameters that represent background viscosity and diffusivity, respectively. In this study and in selected simulations these two parameters are increased in comparison to the modern standard setting. The rationale is that an Arctic Ocean with less sea ice than today is governed by fundamentally different dynamics of heat and momentum exchange between the ocean and atmosphere. For example, the presence of enhanced eddy kinetic energy in regions of low sea ice cover (Von Appen et al., 2022) and weakened Arctic stratification due to enhanced shear-driven turbulent mixing in regions where atmosphere and ocean interact more intensely under reduced sea ice conditions (Polyakov et al., 2020). Yet, we note that during past warm climates also other latitude bands than the Arctic may have experienced conditions favourably to more enhanced ocean

https://doi.org/10.5194/egusphere-2026-4723
Preprint. Discussion started: 18 August 2026

vertical mixing (e.g., Lohmann et al., 2022). By implementing increased vertical ocean mixing in COSMOS, Lohmann et al. (2022), who also provide a more detailed explanation of the modelling methodology this study is built on, observed strong polar warming and reduced seasonality, in particular at high latitudes. We note here that from the three different mixing settings employed by Lohmann et al. (2022) we only consider the one with the weakest modification of background parameters. Even at this weak increase of parameter values the model version with enhanced ocean vertical mixing shows strong warming and much reduced Arctic summer sea ice. This finding is consistent with previous work studying the impact of ocean vertical mixing on the Arctic in a modern climate and based on a different modelling system (Liang and Losch, 2018). The enhanced-mixing experiments employed by us are not intended as a direct estimate of Early Pliocene diffusivity, but as a sensitivity experiment testing the climatic impact of unresolved ocean mixing processes within physically plausible bounds.

3.3 Model spinup and data treatment

Here, by employing global coupled atmosphere-ocean-land surface simulations that are part of, or related to, the PlioMIP2 (Haywood et al., 2016) and MioMIP (Burls et al., 2021a) simulations performed with COSMOS (Stepanek et al., 2020; Lohmann et al., 2022; Hossain et al., 2020), we analyze different past warm climate states. Modelled sea ice concentration (SIC, in %), sea ice thickness (SIT, in m), SST (in °C), and near-surface air temperatures (SAT, in °C) is compared to available Arctic marine sites and terrestrial Pliocene/Miocene sections. For each simulation, we have spun up the model for 1,850 model years. Thereafter, we evaluate the following 100 years of model output regarding the analyses presented here.

For the presentation of results in the following section, we note that spatial resolution on the employed ocean grid has appreciable regional bias in the Atlantic-Arctic realm (Fig. 3). Therefore, except for ocean meridional streamfunction, that is model-internally already brought to a regular latitude-depth grid, all ocean model outputs have been interpolated (conservative

https://doi.org/10.5194/egusphere-2026-4723
Preprint. Discussion started: 18 August 2026

remapping; Climate Data Operators (CDO), Schulzweida et al., 2023) to a regular grid before conducting analyses presented in this manuscript. An exception to this rule is point-wise interpolation of ocean- and sea ice conditions to geographic core location. Here, inverse distance weighted interpolation (CDO) has been applied directly to data on the original ocean grid. Choice for the interpolation algorithm at core location is accommodating the derivation of interpolated information at ODP Site 910 close to the coastline in the Miocene ocean model setup. There, traditional conservative or bilinear interpolation algorithms would lead to unavailability of quantitative information at a core location. Target resolution of spatially resolved interpolations is 1x1°, except for data used in a model data comparison with other CMIP models, where we employ a finer quarter-degree target resolution for comparison with models that have very different, and partly much higher, spatial resolution.

To better understand dynamics that lead to the simulated sea ice, ocean temperature and air temperature states, we also analyze heat flux between ocean and atmosphere and overturning streamfunction. Furthermore, we derive implied meridional heat transports that are useful for tracing the pathway heat towards the Arctic. We compute implied meridional heat transport for the total atmosphere-ocean system (Equ. 1) as well as separately for the ocean (Equ. 2) and the atmosphere (Equ. 3). To this end, we zonally integrate the monthly mean net top-of-the-atmosphere radiative imbalance (Equ. 1) and the net heat flux between ocean and atmosphere (Equ. 2), both conservatively interpolated to a regular grid, and accumulate the result meridionally from the North Pole southward to latitude φ. This construction assumes closure of the energy balance, as is inherent to the definition of an implied heat transport. For the atmosphere (Equ. 3) we derive the result as the residual between implied total and oceanic heat transports. We deliberately depart from the common convention of integrating from south to north (Trenberth and Caron, 2001) when deriving the cumulative meridional heat transport across

https://doi.org/10.5194/egusphere-2026-4723
Preprint. Discussion started: 18 August 2026

latitudes. Because our study focuses on the Arctic, we consider closure of the energy budget there to be more important than achieving closure in the Southern Hemisphere and integrate rather from north to south. By construction, this ensures that the heat transport at the North Pole is exactly zero, even in the presence of non-zero residual trends in the oceanic and atmospheric energy budgets as generally the case in climate simulations.

$$MHT_{total}(\varphi) = \int_{-90}^{\varphi} (R_{SW} + R_{LW})\, dA_{atm} \quad (1)$$

$$MHT_{ocean}(\varphi) = \int_{-90}^{\varphi} F_{oa}\, dA_{ocean} \quad (2)$$

$$MHT_{atm}(\varphi) = MHT_{total}(\varphi) - MHT_{ocean}(\varphi) \quad (3)$$

Here, φ denotes latitude, and MHT_{total}, MHT_{ocean}, and MHT_{atm} represent the total, oceanic, and atmospheric meridional heat transport, respectively. R_{SW} and R_{LW} are the net shortwave and net longwave radiative fluxes at the top of the atmosphere, and F_{oa} is the net heat flux across the atmosphere–ocean interface. dA_{atm} and dA_{ocean} denote the area of atmosphere and ocean grid cells in the meridional integration.

When discussing effects of simulations with and without enhanced ocean vertical mixing we address the potential problem of a seasonal offset between sea ice distribution and SST seasonal minima and maxima (Khoo et al., 2025). For our analysis, we therefore consider the winter/spring and summer SIC seasons as January–May and May–September, respectively. Furthermore, for a description of COSMOS model performance in comparison to other models (see Section 4.1) we consider boreal winter (DJF) and summer (JJA) for SST, and cold season (NDJFMA) and summer season (ASO) for SIC. These definitions stem from our model intercomparison of COSMOS to various CMIP models presented previously for the Southern Ocean (Khoo et al., 2025) and are reused here towards enabling a direct comparison of our inferences on COSMOS model performance for the Arctic with that for the Antarctic. When considering the

https://doi.org/10.5194/egusphere-2026-4723
Preprint. Discussion started: 18 August 2026

minimum/maximum of temperature and sea ice we refer to September and March, respectively, in order to reduce the overlap of different expression of seasonality between different months.

3.4 Compilation of CMIP pre-industrial simulations for a model-intercomparison

The COSMOS have been extensively applied across a wide range of Cenozoic climate states (Section 3.1). This makes them a valuable tool for comparative exploration of Earth's climate's response to different forcings, boundary conditions, and feedbacks. To contextualize our inferences about Arctic environmental conditions within the broader context of climate and palaeoclimate research we perform a comparison of key metrics of simulated pre-industrial control (*piControl*) warm- and cold-season Arctic SIC and SST with findings from other climate models. Here, we focus on the North Atlantic to Arctic Ocean as the primary region of interest. . As benchmark we use similar simulations prepared with various CMIP5 and CMIP6 models available from the Earth System Grid Federation (Cinquini et al., 2014; https://esgf-metagrid.cloud.dkrz.de/). Respective results in Figs. 4-7 are presented at a common regular quarter-degree grid to accommodate various different model resolutions in the various CMIP iterations while maintaining the presentation of high spatial detail in the Arctic from individual simulations. Since the COSMOS has emerged within the generation of CMIP5 models, a fair comparison of models should focus on the CMIP5 ensemble. Yet, to bridge the gap to more recent modelling efforts, and to make our results also interpretable in the context of newer paleoclimate models, we also present a comparison of the COSMOS' pre-industrial climate to the CMIP6 ensemble of *piControl* simulations. Our compilation of available CMIP model output – including the specific models and datasets used here for the preindustrial-related part of the intercomparison – has been presented and documented in detail in the framework of the study by Khoo et al. (2025), who compare the COSMOS to other CMIP (and PMIP) models with a focus

https://doi.org/10.5194/egusphere-2026-4723
Preprint. Discussion started: 18 August 2026

on Southern Hemisphere high latitudes, specifically the Weddell Sea across the Holocene, the Last Glacial Maximum, and the Last Interglacial; readers interested in that perspective are referred to their supplement. Here, we perform the equivalent analysis for the Arctic for pre-industrial conditions, applying the same season definition as outlined in Section 3.3 (following Khoo et al., 2025). Taken together, both studies document performance of the COSMOS for polar sea surface temperature and sea ice conditions in relation to models from CMIP5 and CMIP6.

4 Results

Our modelling results are based on climate model output that has been simulated with established boundary conditions for the pre-industrial (PI), the mid-Piacenzian (~3 Ma) (mPLIO) (Dowsett et al., 2016), and the Miocene (~15 Ma) (MIO) (Hossain et al., 2020). By employing a multi-proxy, multi-parameter, multi-site model-proxy comparison, covering the periods from the Late Miocene to the Late Pliocene, we evaluate the impact of non-resolved processes in the ocean model that would warm the Arctic via enhanced ocean vertical mixing. To this end we quantify the quality of proxy-model agreement on the seasonal cycle of sea ice in simulations at the AAG with and without enhanced vertical mixing, thereafter extending the analysis to the wider Arctic realm across the Pliocene-Miocene by considering additional proxy sites. First, however, we evaluate the realism of the pre-industrial Arctic sea-ice distribution and sea surface temperatures simulated by COSMOS through comparison with published datasets from different generations of CMIP. This provides a broader context for interpreting our modelling results within palaeoclimate modelling, where climate models with substantially different characteristics from COSMOS are widely used (Stepanek et al., 2020; Haywood et al., 2020).

https://doi.org/10.5194/egusphere-2026-4723
Preprint. Discussion started: 18 August 2026

4.1 Model intercomparison for pre-industrial climate and implications for Early Pliocene warmth

With a documented climate sensitivity of 4.7°C per doubling of carbon dioxide, a metric that is minorly impacted by background geography and climate (Stepanek et al., 2020), the COSMOS are at the warmer end of the likely range of climate sensitivity published for both the CMIP5 generation of climate models, as assessed in the Intergovernmental Panel on Climate Change (IPCC) Fifth Assessment Report (AR5) (Flato et al., 2014), and the CMIP6 generation, as assessed in the IPCC Sixth Assessment Report (AR6) (Sherwood et al., 2020). To place our findings on COSMOS's performance in simulating a "blue Arctic" in the broader context of climate modeling, we compare its simulation of the pre-industrial Arctic climate with corresponding results from other CMIP models. We find that the COSMOS simulates Arctic sea surface temperatures and sea ice distribution in line with other pre-industrial simulations based on similar resolution and model generation (Figs. 4-7). In comparison to both the CMIP5 and CMIP6 ensembles, the COSMOS simulate a comparably compact PI Arctic cold season sea ice distribution (NDJFMA, Fig. 4). There are only minor regions of disagreement between the simulation of Arctic sea ice beyond the 2σ-threshold of all models (e.g. north of Greenland and in the Canadian Arctic Archipelago for CMIP6; Fig. 4). In the following we address different definitions of seasons for SST and SIC since seasonality between sea ice and ocean surface temperature is shifted. Boreal winter (DJF) SST (Fig. 5) illustrates relatively limited cold season sea ice extent in COSMOS linked to more pronounced extension of Atlantic warmth towards the Arctic. The entire region between ODP Site 642, ODP Site 907, and ODP Site 910 is warmer than the CMIP ensemble mean. Site locations considered here for a comparison of modelled and reconstructed climate (Fig. 1) are mostly outside regions where COSMOS deviates from the simulated SST and SIC of both CMIP5 and CMIP6 ensembles. With respect to the CMIP6

https://doi.org/10.5194/egusphere-2026-4723
Preprint. Discussion started: 18 August 2026

ensemble, largest deviations are found in the region between Bering Strait and the Canadian Arctic to Labrador Sea on the one hand, and in the region between ODP Site 907 and Svalbard on the other hand (Fig. 5). The latter deviation occurs in the presence of substantial model-spread in CMIP. Boreal summer sea ice (ASO; Fig. 6) is in the COSMOS more compact, in particular in the western region of the AAG. Regions of deviation are constrained to the north of Greenland and the Canadian Arctic Archipelago, and are found near the coast of Chukchi Sea to Beaufort Sea in comparison to CMIP6 (Fig. 6). Boreal summer SSTs (ASO) show that, while the COSMOS are a bit colder than the model ensembles in the central Arctic Ocean (Fig. 7) and show substantial deviation to CMIP6 (but not CMIP5) models, except for the eastern Barents Sea to Kara Sea, the COSMOS largely simulate a warmer North Atlantic to Arctic realm, in particular at the AAG. While the CMIP6 ensemble is more successful in simulating warmer eastern Arctic marginal seas than the CMIP5 ensemble (i.e. around ODP Site 910), the simulated PI boreal summer and winter conditions are in the COSMOS already on the warmer side, suggesting that the COSMOS' cold bias in the Arctic may actually be milder than that identified for other CMIP5 or CMIP6 models (Zhang et al., 2023). This comparison of COSMOS to CMIP model ensembles' PI state of the Arctic indicates that, for recent climate, the AAG in this model is clearly on the warm side.

Drawing on previous findings from PlioMIP, we can extend our assessment of COSMOS's relative performance for the recent Arctic to the Pliocene. COSMOS has been shown to behave similarly to other models participating in PlioMIP with respect to the simulated Arctic climate. It exhibits a comparatively high climate sensitivity (PlioMIP1: Haywood et al., 2013; PlioMIP2: Haywood et al., 2020) and lies within the warmer half of the model ensemble in terms of Arctic conditions (de Nooijer et al., 2020). This provides confidence that the Pliocene Arctic sea surface

https://doi.org/10.5194/egusphere-2026-4723
Preprint. Discussion started: 18 August 2026

temperatures simulated by COSMOS are broadly consistent with those produced by other climate models used in Pliocene climate research and, if anything, tend to be on the warmer side.

Extending this comparison to Pliocene Arctic sea ice, COSMOS simulates a relatively small sea-ice extent during the mid-Piacenzian Warm Period compared with other PlioMIP2 models (de Nooijer et al., 2020), a tendency that is even more pronounced relative to the PlioMIP1 ensemble (Howell et al., 2016). Although the PlioMIP2 configuration of COSMOS has a higher equilibrium climate sensitivity (ECS) than its PlioMIP1 counterpart – reflecting the use of dynamic vegetation rather than the prescribed vegetation employed in PlioMIP1 and highlighting the influence of modelling methodology on simulated Pliocene warmth – PlioMIP2 also includes a larger number of models with relatively high ECS. Consequently, the ensemble-mean reduction in Pliocene Arctic sea-ice extent relative to the pre-industrial is greater in PlioMIP2 than in PlioMIP1, a pattern that is likewise reproduced by COSMOS (Stepanek et al., 2012; Haywood et al., 2013; Howell et al., 2016; de Nooijer et al., 2020; Haywood et al., 2020; Stepanek et al., 2020).

Another aspect impacting the degree of warmth in the Pliocene Arctic is the state of the CAS. The exact timing of the gateway's closure is, however, uncertain (Montes et al., 2015; Haug and Tiedemann, 1998; Osborne et al., 2014). The shoaling of the CAS to <100 m water depth at 4.6 million years ago (Haug and Tiedemann, 1998) coincides with intensification of the Gulf Stream and the introduction of warmer and more saline water masses to high northern latitudes. The final closure of the CAS occurred prior to the intensification of Northern Hemisphere glaciation, around 2.7 million years ago (Sarnthein et al., 2009; Bartoli et al., 2005; Osborne et al., 2014). A modelling study where the CAS was closed during the Early to Late Pliocene led to a warmer Arctic (Lunt et al., 2008b), which is explicitly considered by our Late Pliocene model setup.

https://doi.org/10.5194/egusphere-2026-4723
Preprint. Discussion started: 18 August 2026

Extending this analysis to the Miocene, we find that in the MioMIP1 the COSMOS produce Arctic temperature anomalies (both for SST and SAT) that are consistently among the warmest in their respective groups presented by Burls et al. (2021b). We note, however, that a direct comparison of models with each other is more difficult in MioMIP1 owing to differences in geographies and carbon dioxide levels employed. Nevertheless, these results suggest that also for the Miocene we can assume that the climate states derived by means of the COSMOS may be among the closest matches of modelled Arctic conditions (that generally are warmer than models suggest) in comparison to proxy data.

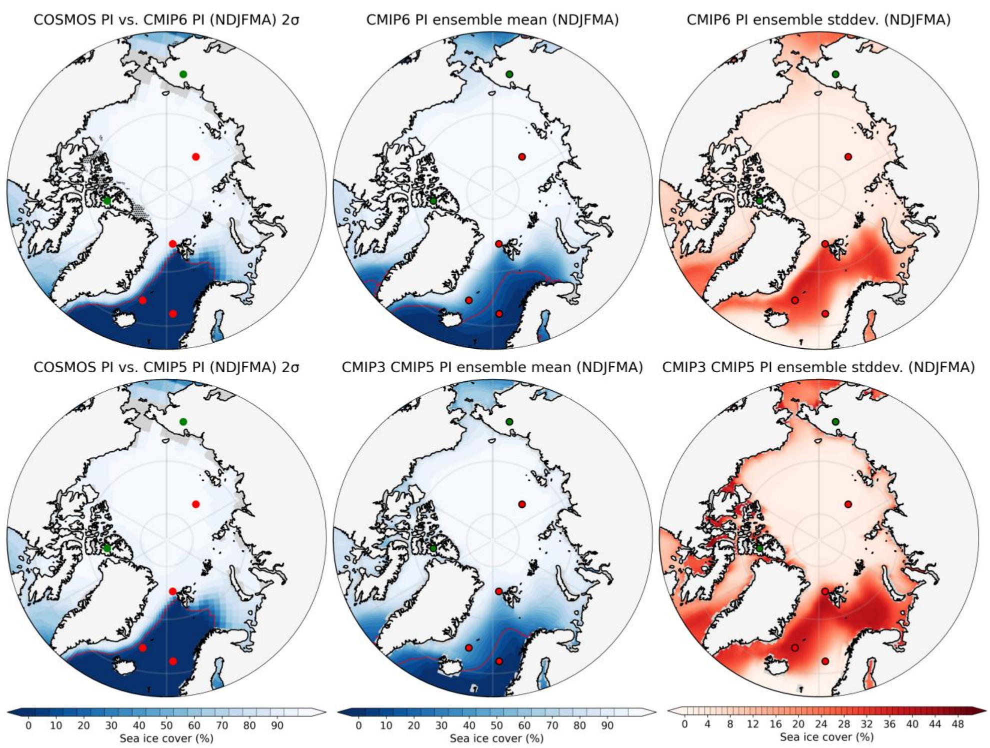

Figure 4. Model-intercomparison. Comparison of boreal cold season (NDJFMA) PI SIC simulated with COSMOS (left column) in comparison to CMIP5- (bottom) and CMIP6-class (top) models. CMIP

https://doi.org/10.5194/egusphere-2026-4723
Preprint. Discussion started: 18 August 2026

ensemble means (without COSMOS, middle column) and ensemble standard deviation (stddev) (right column) shown for reference. In the left column, disagreement between COSMOS and the ensemble beyond a 2σ-treshold indicated by stippling. Differences in land-sea masks shown in dark grey, modern observed coastlines and continents shown by black lines and light gray shading, respectively. Location of proxies included in the model-data comparison indicated by red (ocean) and green (land) circles, see text for details. Purple lines in left and middle columns show the sea ice border (15%-isoline) for COSMOS and CMIP ensembles, respectively.

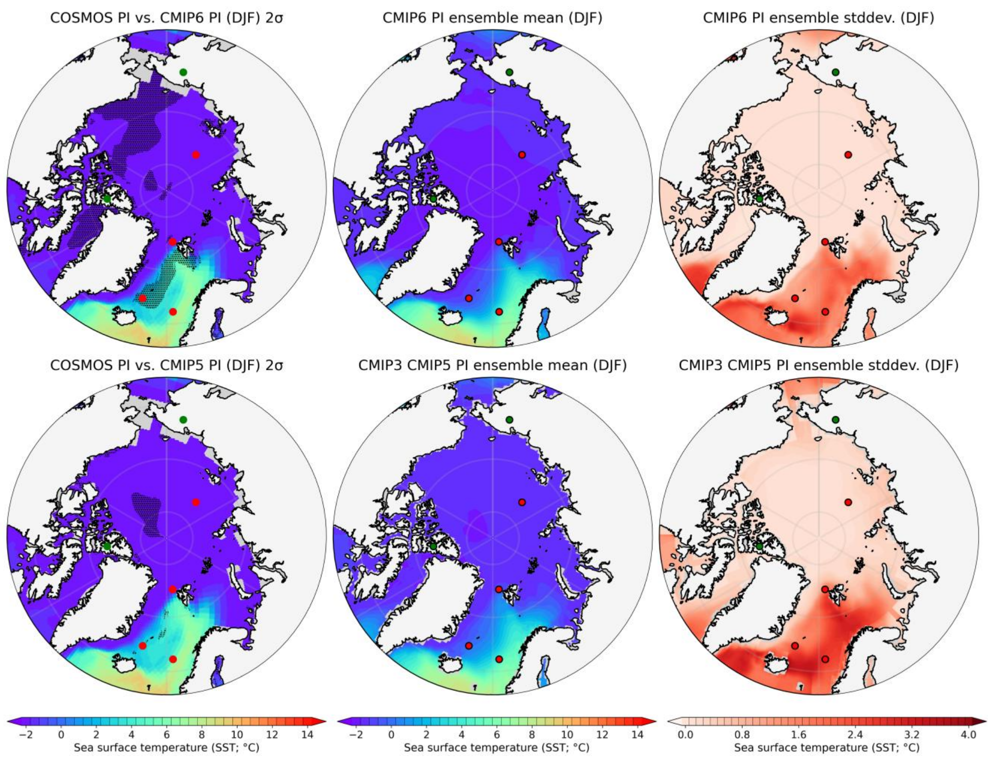

Figure 5. Model-intercomparison. As Figure 4, but for boreal winter (DJF) SST.

https://doi.org/10.5194/egusphere-2026-4723
Preprint. Discussion started: 18 August 2026

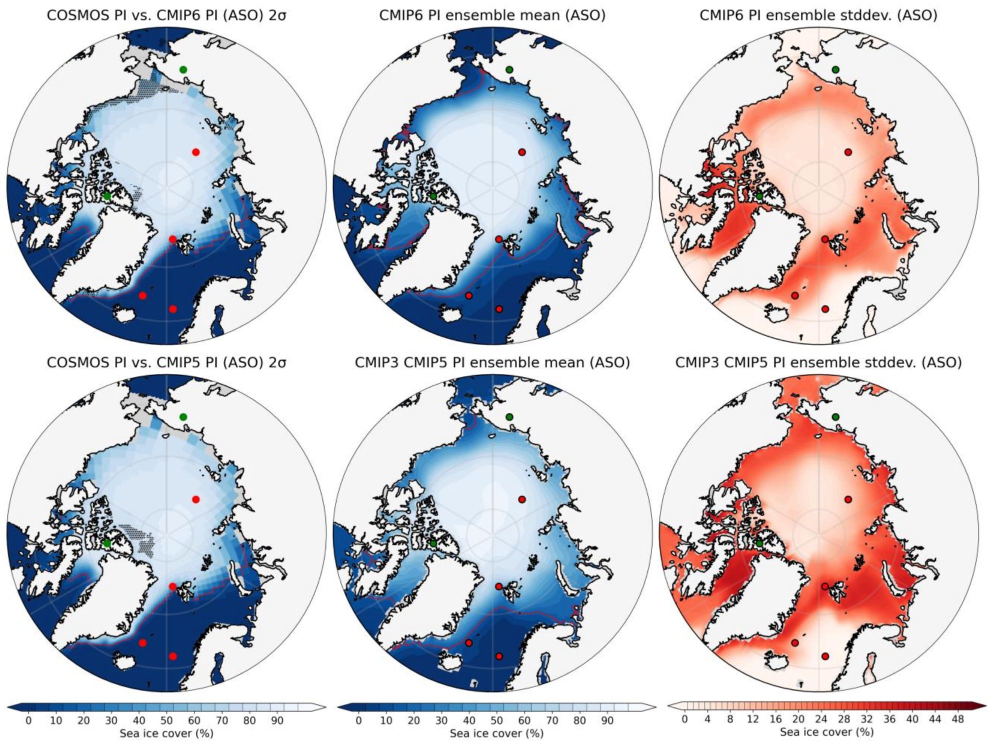

Figure 6. Model-intercomparison. As Figure 4, but for boreal sea ice summer season (ASO) SIC.

https://doi.org/10.5194/egusphere-2026-4723
Preprint. Discussion started: 18 August 2026

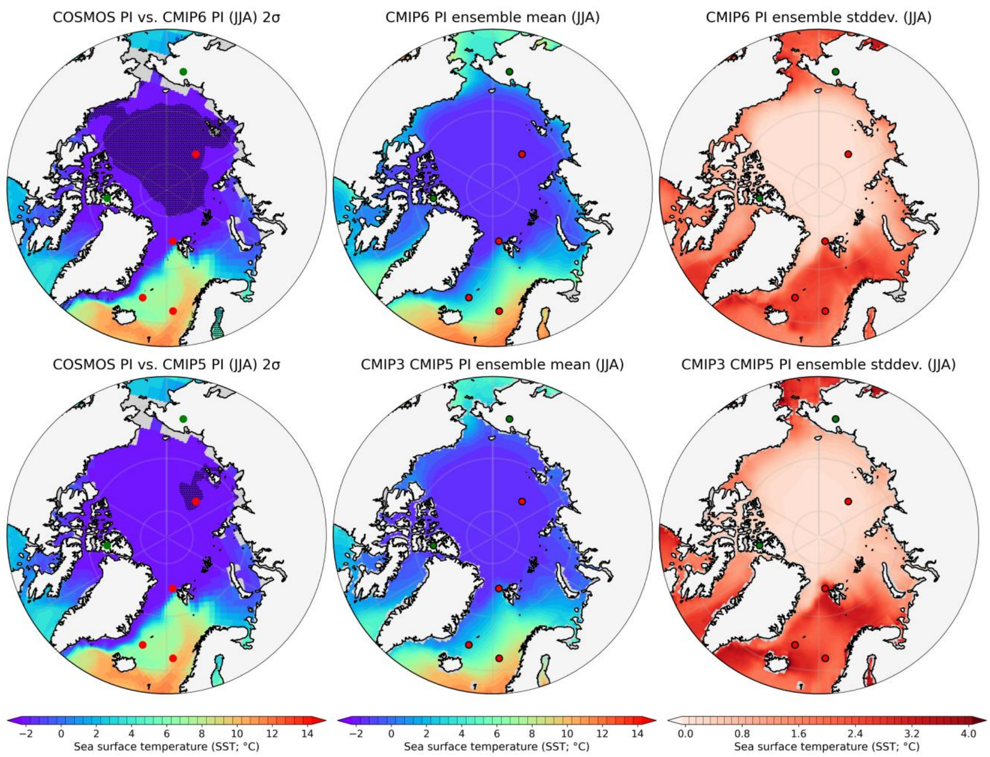

Figure 7. Model-intercomparison. As Figure 4, but for boreal summer (JJA) SST.

The fact that even the comparably warm COSMOS are unable to reproduce reconstructed warm and low Arctic sea ice conditions of the mid-Piacenzian Warm Period (de Nooijer et al., 2020) and the warm Arctic of the Miocene (Burls et al., 2021b), suggests that this model is a suitable example to highlight the importance of mechanisms that could increase simulated warmth towards plausibly reconciling models and proxy reconstructions (De Nooijer et al., 2020; Howell et al., 2016). This suggests that model–proxy discrepancies in our simulations of Late Pliocene to Late Miocene Arctic SST and SIC, both at the location of ODP Site 910 and across the wider Arctic, may reflect a systematic underestimation of North Atlantic and Arctic warmth in climate-model simulations of past warm periods relative to geological proxy reconstructions. These

https://doi.org/10.5194/egusphere-2026-4723
Preprint. Discussion started: 18 August 2026

findings underscore the need to better understand causes of model–data discrepancies in the Arctic. With this study, our analysis focuses on the potential role of missing or inadequately represented processes in climate models, and in particular the choice of ocean vertical mixing parameters, which has been identified as a key control on high-latitude climate and sea ice (Zhang and Steele, 2007; Allende et al., 2024; Lohmann et al., 2022).

4.2 Testing a "blue" Arctic for the Early Pliocene with a numerical approach

Based on the proxy-based findings documented in Figure 2 and acknowledging the uncertainty in the Early Pliocene paleoceanography of the central Arctic Ocean, we test the hypothesis of a summer sea-ice-free ("blue") Arctic Ocean during the Early Pliocene by performing several sensitivity experiments with COSMOS as described in Section 3 (Stepanek et al., 2020). Our climate model data set consists of five simulations (Table 1) that cover the pre-industrial (PI) period at 280 ppm CO_2, the mid-Piacenzian (~3 Ma) at 400 ppm CO_2 and the middle Miocene (~15 Ma) at 450 ppm CO_2, respectively, complemented by dedicated additional simulations with enhanced vertical ocean mixing that increase northward heat transport and remove some of the cold bias (Lohmann et al., 2022). Together, these simulations provide a climatic representation of comparably cold (pre-industrial), warm (Pliocene with standard ocean vertical mixing), and very warm (Miocene with standard ocean vertical mixing, and Pliocene and Miocene with enhanced ocean vertical mixing) conditions in the Arctic that can be tested against the climate proxy data for the Early Pliocene compiled in Figure 2. Specifically, we find that, although, under standard mixing, COSMOS is able to reproduce a global mid-Piacenzian climate that is ~3°C warmer than today and shows appreciable Arctic amplification (Stepanek et al., 2020), it has difficulties reproducing the strongly-reduced meridional temperature gradient that has been inferred from proxy records (Dowsett et al., 2013). The effects of enhanced ocean vertical mixing in our

https://doi.org/10.5194/egusphere-2026-4723
Preprint. Discussion started: 18 August 2026

simulations include an increase in the heat capacity of the Earth System (Lohmann, 2020) and a reduced meridional temperature gradient in combination with a warmer deep ocean (Lohmann et al., 2022). The warming effect of a closed Central American Seaway (CAS) on the Arctic, which has been shown to promote warmer Arctic conditions (Lunt et al., 2008b; see Section 4.1), is already incorporated in our Pliocene simulations through the presence of an intact Isthmus of Panama and is therefore also accounted for in our model-data comparison.

Table 1: Climate simulations employed for the study of Arctic sea ice and sea surface temperature, spanning the periods Miocene, Pliocene, and pre-Industrial (PI). Details of model setups are described in the text and are based on information from referenced literature (Hossain et al., 2020; Lohmann et al., 2022; Stepanek et al., 2020; Stärz et al., 2017). We consider the climatic impact of atmospheric carbon dioxide concentrations (CO_2), in the range from 280 ppm to 450 ppm, and of ocean vertical mixing at modern standard and at enhanced intensity. Enhanced mixing refers to an increase in the values of background viscosity and background diffusivity by a factor of five. This is the lowest value considered in previous work (Lohmann et al., 2022). Simulations are attributed with a subjective categorization of the state of the Arctic, ranging from cold via warm to very warm climates. For reference, we list in brackets simulated absolute average SST (°C) in the Arctic (>66°N) for annual mean, boreal winter (Dec-Feb), and boreal summer (Jun-Aug), respectively. Prior to computation of these measures, simulated climate data has been interpolated from the native ocean model grid to a regular 1x1° resolution using a conservative remapping algorithm. Annual mean meridional temperature gradients in the Northern Hemisphere (MTG) from (Lohmann et al., 2022). More information on large-scale temperature and sea ice patterns available from (Lohmann et al., 2022), in particular their Table 2.

https://doi.org/10.5194/egusphere-2026-4723
Preprint. Discussion started: 18 August 2026

Simulation	**Time reference**	**Geography, most relevant differences from modern in this study**	**CO_2 (ppm)**	**Ocean mixing**	**Arctic climate**	**MTG /°C**
PI	recent climate	modern	280	standard	cold (-0.73; -1.03; -0.34)	42.8
mPlio^{400}	mid-Piacenzian (~3.0 Ma)	PRISM4 (Dowsett et al., 2016)), closed Bering Strait	400	standard	warm (1.15; 0.04; 2.58)	37.7
mPlio$^{400}_{mix}$	mid-Piacenzian (~3.0 Ma)	PRISM4 (Dowsett et al., 2016)), closed Bering Strait	400	enhanced	very warm (1.72; 0.29; 3.62)	36.0
Mio^{450}	middle Miocene (~15 Ma)	(Herold et al., 2008) with adaptations, open Central American Seaway	450	standard	very warm (2.18; 0.36; 4.36)	37.7
Mio$^{450}_{mix}$	middle Miocene (~15 Ma)	(Herold et al., 2008) with adaptations, open Central American Seaway	450	enhanced	very warm (2.40; 0.58; 4.98)	37.0

In Figure 8, we present a multi-proxy, multi-epoch comparison of simulated and reconstructed conditions of the Arctic at the Miocene-Pliocene boundary. Here we compare proxy data from different stages of the Miocene-Pliocene period with climate simulations of the respective time slice. By evaluating both simulations with standard modern and enhanced ocean vertical mixing parameter settings, we quantify the impact of enhanced ocean vertical mixing on the agreement between climate model simulations and geological record. The results in Figure 8 show that across the wider Arctic realm the presence of enhanced ocean vertical mixing greatly improves the agreement between reconstructed and simulated climate across the period from the Late Miocene to the Late Pliocene. In contrast, simulations using standard modern background mixing

https://doi.org/10.5194/egusphere-2026-4723
Preprint. Discussion started: 18 August 2026

parameters, despite incorporating elevated CO_2 concentrations and reconstructed paleogeographic boundary conditions, predict relatively moderate oceanic and near-surface atmospheric warming and sea ice reduction relative to the pre-industrial control state. These simulations fail to reproduce the degree of warming inferred from the geological record. While the amplitude of the reduction in model-bias vs. reconstruction is dependent on region, period and proxy-archive, in our model enhanced vertical mixing in the ocean unequivocally leads to increased SST and SAT and reduced sea ice at all available proxy sites. For Late Miocene Central Arctic Ocean August SST at PS87/106, annual SST for Early and Late Pliocene at ODP 907A, and for terrestrial proxies at El'gygytgyn and Beaver Pond, the reduction of the underestimation of SST/SAT is in the range of 11% - 20% (Fig. 8). Warming is widespread in the range of 1-2°C and, thus, substantial. At ODP Site 907 in the Nordic Seas (Fig. 1), where our model simulations do not indicate presence of substantial amounts of sea ice in either Early Pliocene or Late Miocene winter or summer, the consideration of increased ocean vertical mixing nevertheless reduces the model-proxy mismatch by 0.7°C (Fig. 8). In the AAG region (ODP Site 910) we find a profound impact of enhanced ocean vertical mixing on spring sea ice (72% reduction), while the reconstruction suggests no presence of sea ice (indicated by a lack of the respective bar being shown; cf. Fig. 8, bar plot for location ODP 910). Indeed, only the simulation with enhanced ocean vertical mixing leads to an absolute sea ice concentration below 15%, which we consider as ice free conditions. While there is a lack of central Arctic temperature records for the Early Pliocene, we find that for the Late Miocene at site PS87/106 (Stein et al., 2016) SSTs are increased by 1.3°C if enhanced ocean vertical mixing is considered in our model (Fig. 8). In north-eastern Siberia at Lake El'gygytgyn (Brigham-Grette et al., 2013) we find that Early Pliocene warmest month SAT is increased by 1.5°C when enhanced ocean vertical mixing is considered (Fig. 8). For the reconstruction from the proxy site Beaver Pond on Ellesmere Island (Fig. 1) the simulation with enhanced mixing approaches the reconstructed Early Pliocene warm

https://doi.org/10.5194/egusphere-2026-4723
Preprint. Discussion started: 18 August 2026

season SAT within the documented proxy uncertainty range. These results demonstrate that processes in climate models that lead to a warmer Arctic via more vigorous mixing of the ocean are viable candidates for exploring causes of model-proxy mismatches in past warm Arctic climates. Our results also suggest that the sensitivity of simulated climate to enhanced ocean vertical mixing is particularly strong for regions proximal to seasonal sea ice limits at the AAG, where related feedbacks play a larger role.

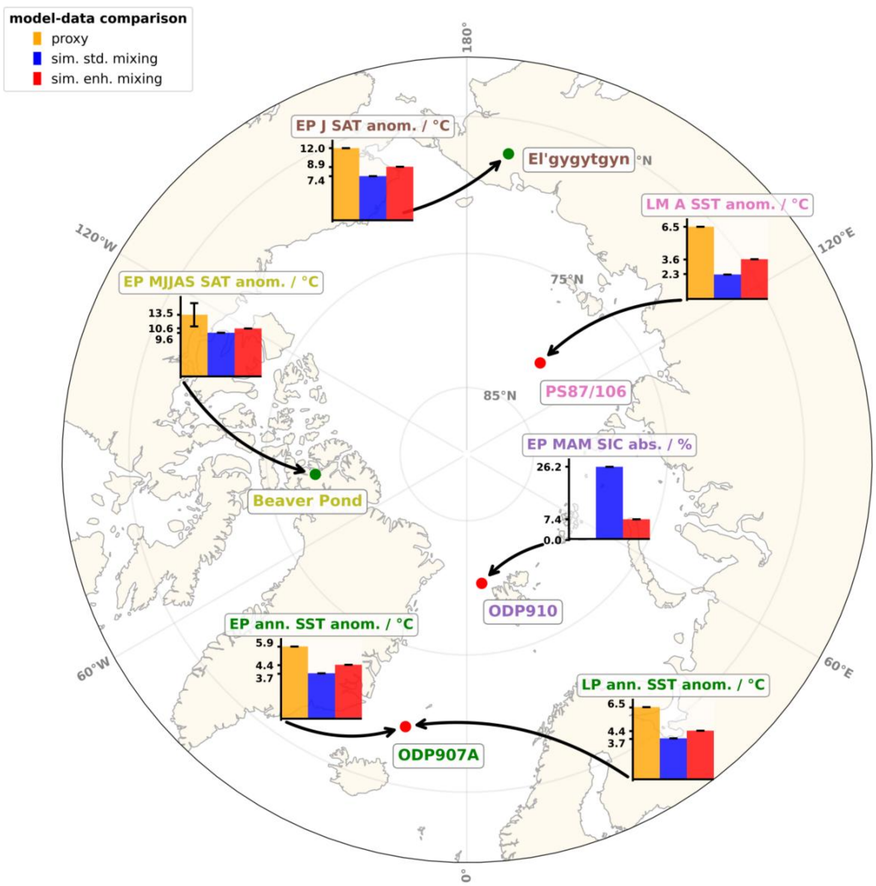

https://doi.org/10.5194/egusphere-2026-4723
Preprint. Discussion started: 18 August 2026

Figure 8. Multi-period, multi-proxy, and multi-parameter model-data comparison in the wider Arctic realm across the Pliocene to Miocene. Considering both marine (red circles) and terrestrial (green circles) proxy-sites we show the degree of agreement between reconstructed (yellow bars) (Herbert et al., 2016; Knies et al., 2014a; Csank et al., 2011a; Csank et al., 2011b; Stein et al., 2016; Brigham-Grette et al., 2013) and modelled environmental conditions in simulations with standard (blue bars) and enhanced vertical mixing (red bars). Environmental conditions considered in our comparison include absolute (abs.) or anomalies wrt. to recent conditions (anom.) of sea ice concentration (SIC, %), sea surface temperature (SST, °C) and surface air temperature (SAT, °C) for Late Miocene (LM), Early Pliocene (EP), and Late Pliocene (LP). Model comparison is performed strictly within Pliocene and Miocene epochs, respectively. This means that an Early Pliocene reconstruction is compared to the simulation from the PlioMIP framework, i.e. to the mid-Piacenzian Warm Period. Analyzed months or seasons of modelled environmental conditions have been selected in agreement with seasonal attribution of the reconstruction as documented for the respective proxy data point. The periods shown here refer to March-May (MAM), March-September (MJJAS), July (J), August (A), or annual mean (ann.). Scales of bar plots differ between shown proxy sites, with the maximum magnitude of bar plots at each proxy location being defined by the height of the largest bar, proxy or modelled. Placement of bar plots on the maps is arbitrary and optimized for contrast with the background map, that represents the observed modern continental outline. Affiliation of a bar plot to a specific core location is indicated by arrows.

4.3 Seasonal sea ice and temperature variability at the AAG (ODP Site 910)

Turning to the AAG, where we have inference on both reconstructed SST and SIC, we can shed more light on the impact of enhanced ocean vertical mixing on the modelled seasonal cycle of these quantities. Results from climate simulations obtained at ODP Site 910 can reproduce the proxy-based climate only with specific boundary conditions. The annual pre-industrial SIC (50-90 %), SIT (~1-2 m) and SST (~ -2ºC) model results (Fig. 9) correspond to modern and proxy-based observation in the eastern Fram Strait (Pieńkowski et al., 2021). However, drastically different conditions are simulated for the mPLIO and MIO experiments with various forcings, yet showing small but distinct differences (Fig. 9). Simulation results with CO_2 forcing of 400 ppm and 450 ppm for Pliocene and Miocene, respectively, suggest winter/spring (January–May) SIC of 10–40% and SIT of < 0.4 m at ODP 910 (Fig. 9), yet ice-free conditions only during summer months (May–September). With enhanced ocean vertical mixing both SIC and SIT are reduced (to <10% and 0.1 m, respectively), reflecting more effective transport of heat from low to high latitudes and stronger local processes fostering warming. The inclusion of enhanced ocean vertical mixing thus mitigates the well-known cold bias of climate models with respect to the geologic record (Dowsett et al., 2013). While the model results from mPLIO400 and MIO450 with standard vertical mixing predict up to 40% sea ice coverage in spring, very much reduced from recent conditions, this is inconsistent with the absence of the spring sea ice proxy IP_{25} in the ODP 910 sediments (Fig. 2). On the other hand, the simulations forced with enhanced vertical ocean mixing for both the mPLIO and MIO set ups reveal extremely thin (<0.1 m) winter sea ice coverage, with SST varying between 4.7 °C and 0.9 ºC in the coldest month of the year, in line with the sea ice proxy data. Interestingly, in a parallel site (ODP 911) on the Yermak Plateau, very low IP_{25} concentration (0.003 µg/g Sediment) was detected in two out of three samples (Clotten et al., 2019) supporting the presence of some sea ice during the winter months on the Yermak Plateau. Furthermore, proxy-based summer SSTs of 5 to 10 ºC (Fig. 2) are similar to results derived from the mPLIO/MIO simulations with enhanced vertical ocean mixing (max. ~10°C; Fig. 9) whereby, for our mid-Piacenzian Warm Period simulation with standard mixing, the temperatures are rather on the colder side (max. ~8°C).

https://doi.org/10.5194/egusphere-2026-4723
Preprint. Discussion started: 18 August 2026

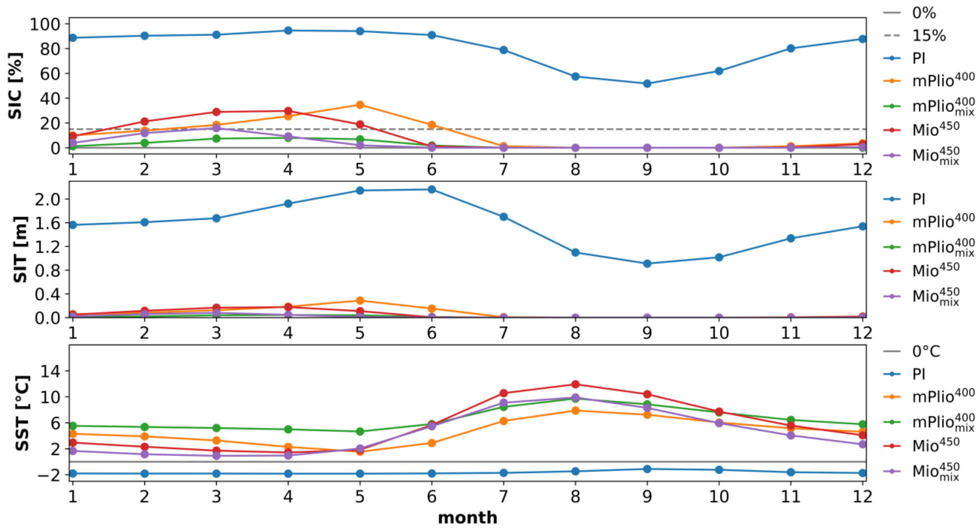

Figure 9. **Seasonal cycle in the Arctic-Atlantic Gateway.** Simulated seasonal cycle of sea ice concentration (SIC; top), sea ice thickness (SIT; middle), and sea surface temperature (SST; bottom) at the location of ODP Site 910 (80.2649ºN, 6.5901ºE) for various simulations with differing geographies (modern, Pliocene, Miocene), mixing parameterizations (standard and enhanced vertical mixing), and carbon dioxide forcing. Simulation names identify the affiliation of a simulation to preindustrial (PI), mid-Piacenzian (mPlio), or middle Miocene (Mio) characteristic geography. Concentrations of carbon dioxide indicated by superscripts following the affiliation key. Simulations, where vertical mixing differs from standard conditions, are identified via the key "mix". See Table 1 for details of model setups. Grey lines indicate 0°C iso-therm, 0 m iso-thickness, and 0% and 15% (sea ice border) iso-concentration, respectively. Data shown in the graph has been interpolated from the native grid of the ocean model to the core's geographic location by employing the inverse distance weighted remapping algorithm (Climate Data Operators; (Schulzweida, 2023).

https://doi.org/10.5194/egusphere-2026-4723
Preprint. Discussion started: 18 August 2026

4.4 A 'blue' Arctic Ocean during the Early Pliocene — Geographic distribution of Arctic sea ice and temperature under enhanced ocean mixing

The simulations that refer to the mid-Piacenzian (~3 Ma) at 400 ppm CO_2, and to the middle Miocene (~15 Ma) at 450 ppm CO_2, both with enhanced ocean vertical mixing (mPlio400mix, Mio450mix), resemble best the climate proxy data at ODP Site 910 for sea ice and SST reconstruction (Figs. 2,9). We propose that by extrapolating findings from both, well constrained model simulations for the entire Arctic Ocean, a consistent environmental scenario for SIC, SIT, and SST can be presented for the Early Pliocene (~4.5 – 5.33 Ma). Figure 10 illustrates these environmental conditions for both winter (March) and summer (September) for three simulations (PI, mPlio400mix, Mio450mix), respectively. In contrast to the pre-industrial (PI) simulation, which exhibits extensive sea ice concentration (SIC) and sea ice thickness (SIT), the Mio450mix simulation produces notably lower maximum SIT values (d_{max} = 0.8 m), compared to the mPlio400mix simulation (d_{max} = 1.6 m). During the Pliocene (mPlio400mix), the thickest sea ice is found in the East Siberian and Laptev Seas, whereas in the Miocene (Mio450mix), maximum ice thickness shifts towards the central Arctic Ocean and the Greenland margin (Fig. 10). Meridional heat transport into the Arctic Ocean is considerably stronger in winter during the mPlio400mix simulation, due to the enhanced vertical mixing and overturning as we will show in Section 4.5. For both mPlio400mix and Mio450mix simulations, the Arctic Ocean is free of sea ice during summer (September), which supports previous data-model reconstructions for the mid-Pliocene warmth (Ballantyne et al., 2013; Csank et al., 2011c; Ballantyne et al., 2010; Dowsett et al., 2016; Dowsett et al., 2013; Dowsett et al., 1996), while our Pliocene simulation with standard ocean vertical mixing still shows presence of sea ice above the 15% threshold and ample extent of SST below 0°C (not shown).

https://doi.org/10.5194/egusphere-2026-4723
Preprint. Discussion started: 18 August 2026

While the PI reference state shows extensive sea ice concentration in the summer, with SIT in the range of 3 m across large parts of the Arctic Ocean and >8 m in Nares Strait, a "blue" Arctic Ocean during the summer is simulated regardless of the boundary conditions defined for the mPlio400mix and Mio450mix simulations. Maximum warmth is simulated for the Mio450mix, with no SSTs at the freezing point (0°C) across the entire Arctic Ocean (Fig. 10). The results clearly show that, while different boundary conditions (e.g. gateways, carbon dioxide) control the seasonality of sea ice, enhanced ocean mixing in the simulations is critical for the presence or absence of sea ice in the Pliocene Arctic Ocean.

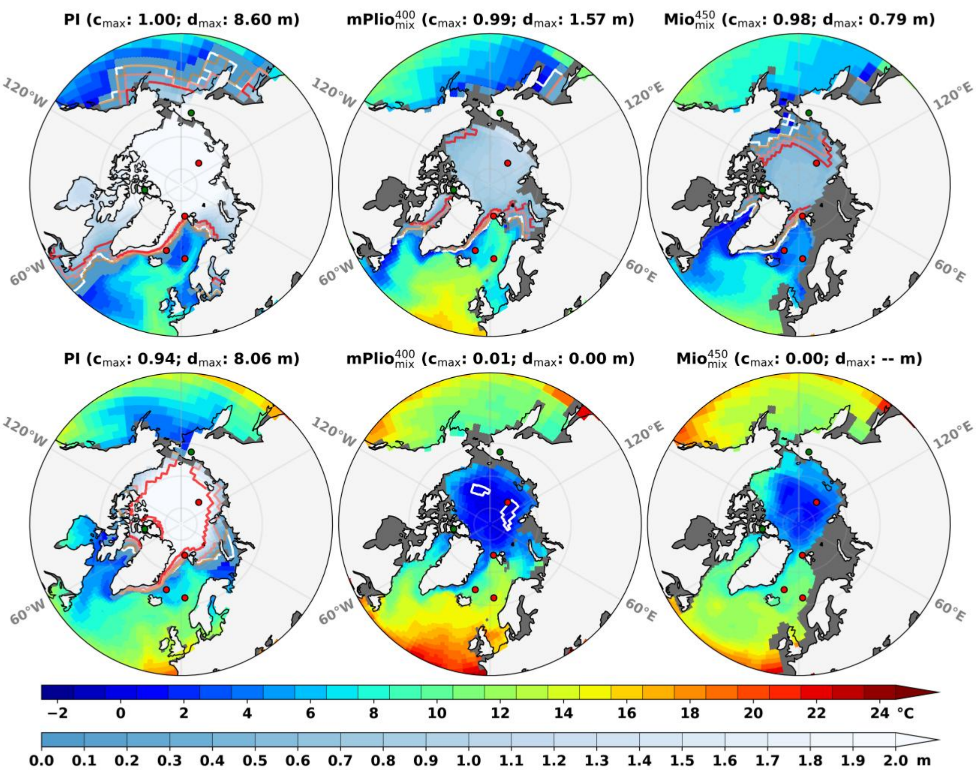

Figure 10. A "blue" Arctic Ocean during past warm periods. Geographic distribution of sea surface temperature (colorful shading), sea ice thickness (blue-white shading), and sea ice concentration (brown,

https://doi.org/10.5194/egusphere-2026-4723
Preprint. Discussion started: 18 August 2026

light red, and dark red iso-lines) for various simulations with differing geographies (modern, Pliocene, Miocene), mixing parameterizations (standard and enhanced vertical mixing), and carbon dioxide forcing. Simulation names identify the affiliation of a simulation to preindustrial (PI), mid-Piacenzian (mPlio), or middle Miocene (Mio) characteristic geography. Prescribed concentrations of carbon dioxide indicated by superscripts following the affiliation key. Simulations with modified vertical mixing identified via the key "mix". See Table 1 for details of model setups. Shown is model output for the region of the Arctic Ocean and for the months of March (upper row) and September (lower row) that has been interpolated from the ocean model's native grid to a regular 1°x1° resolution using the conservative remapping algorithm (Climate Data Operators; (Schulzweida, 2023). Conservative remapping has been chosen to retain details of the model's land-sea-mask. Continents indicated by light gray shading (modern observed) and dark gray shading (model). The isolines shown refer to 0°C isotherm (white), 15% iso-concentration (brown), 50% iso-concentration (light red), and 75% iso-concentration (dark red), respectively. Locations of sites considered in this study indicated by green (for terrestrial) and red (for marine) records, see Fig. 1 and text for details. Unevenness of spatial resolution owes to the ocean model grid, that has high detail in the North Atlantic to Arctic Ocean, but relatively coarse resolution in the North Pacific (see Fig. 3). Maxima of sea ice concentration (c_{max}) and of sea ice thickness (d_{max}) in the entire Northern Hemisphere indicated by annotations in brackets and rounded to two decimals. Ice thickness below 1 mm not shown. For the two months presented here, the results of simulations Mio^{450} and Mio^{450}_{mix} are rather similar, and we only show results for simulation Mio^{450}_{mix}.

4.5 Transport pathways of enhanced-mixing-induced excess heat into the Arctic

Our simulations demonstrate that enhanced ocean vertical mixing consistently increases Arctic warmth across two paleogeographic configurations spanning the Early Pliocene (Table 1), improving the agreement of simulated and reconstructed Arctic conditions in many aspects as described above (Fig. 8). We thereby show that the response of the Arctic Ocean to enhanced ocean vertical mixing is that of an overall warming and reduced sea ice. We now identify

https://doi.org/10.5194/egusphere-2026-4723
Preprint. Discussion started: 18 August 2026

mechanisms that link enhanced ocean vertical mixing in our simulations with increased Arctic Ocean warmth. When analyzing in unison the response of (1) Atlantic Meridional Overturning Circulation (AMOC) (Fig. 11), (2) meridional heat transport in ocean and atmosphere (Fig. 12), and (3) heat exchange between ocean and atmosphere in the North Atlantic to Arctic realm (Fig. 13) in Pliocene and Miocene geographies, we find that the mechanisms behind the response of Arctic sea ice to enhanced ocean vertical mixing fundamentally differ between the Pliocene and Miocene simulations presented here. This difference is linked to the dominant overturning regime in the ocean, Miocene vs. Pliocene.

For the Pliocene we find a clear direct link of enhanced ocean vertical mixing in the ocean, increased strength and expansion of the AMOC, increased strength of northward meridional heat transport in the ocean, and overall increased heat flux from ocean to atmosphere in the North Atlantic to Arctic realm. Enhanced ocean vertical mixing increases, both in strength and depth, the Pliocene North Atlantic Deepwater (NADW) conveyor (Fig. 11), leading to increased heat convergence in the north. The net heat-exchange anomaly between ocean and atmosphere resulting from enhanced ocean vertical mixing is, across most of the North Atlantic–Arctic region, characterised by increased heat transfer from ocean to the atmosphere. An exception are parts of the eastern Arctic Basin, including the Norwegian, Barents, and Kara seas, where the ocean-to-atmosphere heat-flux anomaly indicates that slightly less heat is transferred to the atmosphere under enhanced mixing despite the reduction in sea-ice cover (Fig. 13). For the Pliocene, the impact of enhanced ocean vertical mixing on Arctic climate is therefore a combination of increased northward ocean meridional heat transport (Fig. 12) and local feedbacks, where the latter leads to an overall amplification of the impact of low-latitude heat supply via the ocean route on Arctic warmth in both atmosphere and ocean.

https://doi.org/10.5194/egusphere-2026-4723
Preprint. Discussion started: 18 August 2026

For the Miocene we find a distinctly different process linking enhanced ocean vertical mixing with Arctic warmth. It is evident that the increased mixing leads to a weaker and shallower NADW conveyor belt (Fig. 11). This is directly linked to reduced northward meridional ocean heat transport if compared to conditions in the Miocene setup with standard modern mixing parameters, where the ocean heat transport to the north is already lowered with respect to the pre-industrial setup (Fig. 12). We find not only compensation of reduced northward meridional ocean heat transport by an increase in the respective atmospheric pathway, known as the Bjerknes compensation (Bjerknes, 1964), but we find in fact overcompensation, indicating that the atmosphere route of heat towards the north is much more important with enhanced ocean vertical mixing in the Miocene. In that case, enhanced mixing brings substantial amounts of heat via the atmosphere route towards the Arctic Ocean, which generates substantial warming and, in combination with locally amplifying feedbacks, gives rise to the lowest extent of sea ice found in any of the simulations studied here. In fact, the reduced northward heat transport via the ocean route leads to lower heat content in the Arctic realm in the upper ocean (not shown), highlighting how potent vertical mixing is in distributing heat to the Arctic even indirectly via processes that influence the atmosphere route and local feedbacks.

https://doi.org/10.5194/egusphere-2026-4723
Preprint. Discussion started: 18 August 2026

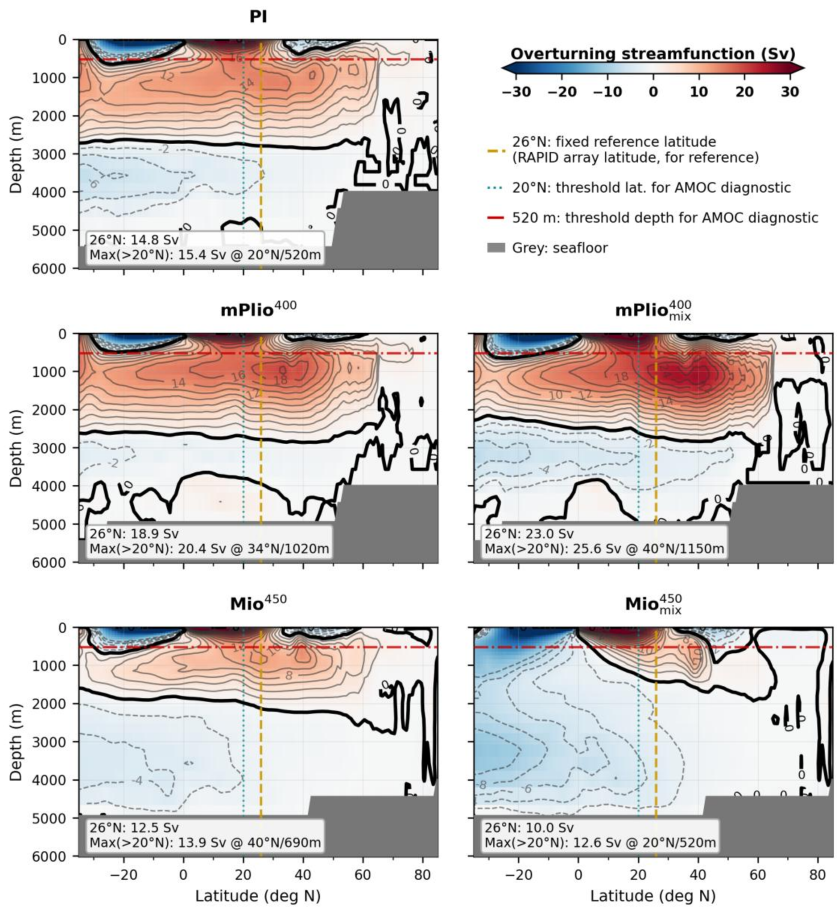

Figure 11. Streamfunction of the Atlantic Meridional Overturning Circulation (AMOC). Zonally integrated meridional volume transport in units of Sverdrup (Sv) shown for various simulations with standard and enhanced ocean vertical mixing. Positive (red hue) values illustrate clockwise circulation from the viewpoint of Europe, while negative (blue hue) values show counterclockwise flow. Upper AMOC cell with clockwise circulation is indicative of the North Atlantic Deep Water conveyor, while the lower AMOC cell with counterclockwise circulation illustrates the inflow of deep water of southern origin, in particular Antarctic Bottom Water. Various AMOC statistics annotated in semitransparent boxes. These values are computed for the region defined by dotted blue (20°N threshold) and dashed red lines, where the latter indicates a depth of 520 m, which is the depth of the first ocean model layer that is fully located

https://doi.org/10.5194/egusphere-2026-4723
Preprint. Discussion started: 18 August 2026

below the commonly assumed 500 m depth threshold for AMOC strength. Bottom topography estimated from the streamfunction (depths below the lowest level where the streamfunction is a finite value unequal to zero).

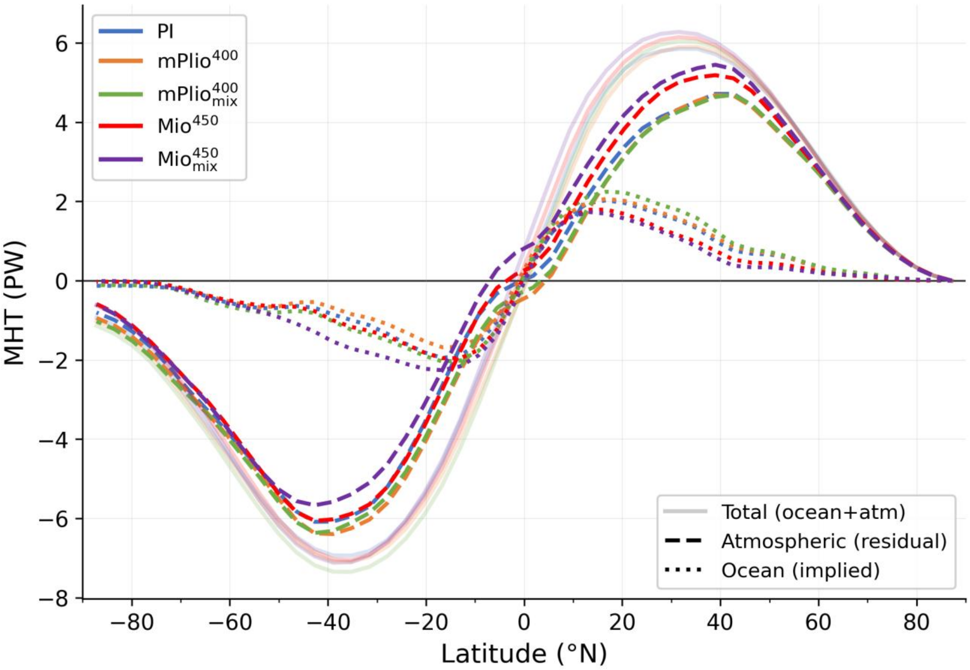

Figure 12. Meridional heat transport (MHT) in ocean, atmosphere, and the total. We show total meridional heat transport in ocean and atmosphere (Total (ocean+atm)) computed from top-of-the-atmosphere radiative imbalance; implied ocean meridional heat transport (Ocean (implied)) derived from ocean-atmosphere heat flux; atmosphere meridional heat transport (Atmospheric (residual)) derived as the difference between both aforementioned quantities. Total transport shown with faint lines to highlight the individual transport routes that are of interest. Transports in units of petawatt (PW) and positive towards the north. See Section 3.3 for details.

https://doi.org/10.5194/egusphere-2026-4723
Preprint. Discussion started: 18 August 2026

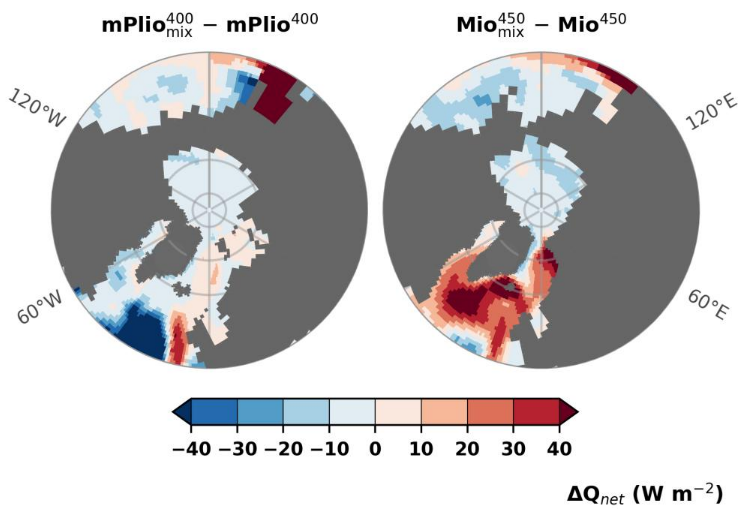

Figure 13. Heat flux anomaly ΔQ_{net} between ocean and atmosphere in the North Atlantic to Arctic realm resulting from enhanced ocean vertical mixing. Shown are anomalies between a simulation with enhanced ocean vertical mixing and the respective reference simulation with standard mixing parameters. Negative values (blue hue) imply increased heat flux from the ocean to the atmosphere, and vice versa. Grey fill indicates the land sea mask in the model for the respective model geography, Pliocene and Miocene, respectively.

5. Discussion

5.1 Enhanced vertical ocean mixing improves Arctic model-proxy agreement

The spring sea ice proxy IP_{25} is absent (below detection limit) in the Early Pliocene (~4.5 – 5.33 Ma) both on the Yermak Plateau (ODP 910) and in the Iceland Sea (ODP 907) (Fig. 2) (Clotten et al., 2019; Knies et al., 2014a). Only after ~4.5-4.0 Ma did a substantial expansion of Arctic sea ice occur. Sea ice reached its modern winter maximum extension in the AAG for the first time during the culmination of the Northern Hemisphere glaciation, ca. 2.6 million years ago (Knies et al., 2014a). This implies that summer sea-ice free conditions prevailed in the eastern AAG only during the Early Pliocene between ~5.3 and 4.5 Ma. Parallel SST values ranging between 5 and 10 ºC in ODP 910 and 8 to 13 ºC in ODP 907 support this inference (Fig. 2). Results from climate simulations obtained at ODP Site 910 can reproduce this climate proxy-based scenario only with specific boundary conditions. The annual pre-industrial SIC (50-90 %), SIT (~1-2 m) and SST (~ -2ºC) model results (Fig. 9) correspond to modern and proxy-based observation in the eastern Fram Strait (Pieńkowski et al., 2021). However, drastically different conditions are simulated for the mPLIO and MIO experiments with various forcings yet showing small but distinct differences (Fig. 9).

In our model, simulations with a comparatively moderate enhancement of vertical mixing (Lohmann et al., 2022) most accurately reproduce sea ice extent and SST reconstructions from the eastern AAG (Fig. 2), the overall warmer Arctic realm suggested by various marine and terrestrial proxies from the late Miocene to the Late Pliocene (Fig. 8), and reconstructed reduced meridional temperature gradients (Lohmann et al., 2022). This suggests that the strength of ocean mixing exerts a greater influence on Arctic sea ice conditions than the prescribed atmospheric CO_2 concentrations alone.

5.2 Physical mechanisms and limitations of enhanced mixing as an explanation

We emphasize that enhanced vertical ocean mixing may compensate for other model limitations in representing key processes related to meridional heat transport, surface albedo and emissivity, the latter two particularly in the Arctic. Among the likely modulators of the Earth's radiative balance – and contributors to Arctic amplification – are cloud cover and atmospheric water vapor, both of which influence regional temperature responses and may help explain a warmer Arctic Ocean (Lohmann et al., 2022). For mPLIO and MIO simulations that are controlled by geography and greenhouse gases alone, it has been found that annual mean cloud cover is globally mostly reduced, but actually increased in the Arctic (Lohmann et al., 2022). In simulations with enhanced ocean vertical mixing, cloud cover is reduced globally and across most of the Arctic but increased closer to the North Pole (cf. Lohmann et al. (2022), their Supplement Figure S9), illustrating the complex pattern of cloud cover changes in a warming Arctic. While in a modern Arctic with pronounced Arctic sea ice the overall annual net-effect of clouds is that of a warming (Intrieri et al., 2002), in a "blue" Arctic with less ice cover we can expect the shortwave radiative impact of clouds, that results in surface cooling, to become more relevant. The net role of clouds in a warmer Arctic, overall warming vs. overall cooling, may therefore depend on model-specific details of cloud properties. The impact of cloud model parameters on the extent of warmth in the Arctic of the Last Interglacial has been recently demonstrated (Akima et al., 2026). Therefore, enhancing the representation of Earth system processes that decrease high-latitude albedo and emissivity — while incorporating the latest insights into Pliocene geographic configurations — could be a viable approach to aligning climate models more closely with the geologic record of past warm Arctic climates.

While the assumed CO_2 alone is able to increase Arctic temperatures in the presence of mPLIO boundary conditions (i.e. mid-Pliocene paleogeography) (Stepanek et al., 2020; Lunt et al., 2008), simulated temperature anomalies are still far too small in comparison to the geological record (Figs. 2,8,9) (Dowsett et al., 2013). Our simulations with enhanced vertical mixing can mitigate this bias. Physical processes that can plausibly be assumed to have mixed the ocean more efficiently during past greenhouse climate states include changes in tidal dissipation due to altered continental and shelf configurations, invigorated tropical atmospheric circulation, and increased storm activity (Fedorov et al., 2013; Lohmann et al., 2022). Alternatively, a reduced meridional temperature gradient, with invigorated warmth in the Arctic, created by vertical

https://doi.org/10.5194/egusphere-2026-4723
Preprint. Discussion started: 18 August 2026

mixing, may only mitigate other model limitations. For example, simulations by Lohmann et al. (2022) have shown that contributions from both planetary albedo and effective emissivity contribute to enhanced warmth at high latitudes. Our results are in line with earlier hypotheses that reduced meridional temperature gradients of the Pliocene resulted from decreased reflectivity of the Earth system and from increased meridional heat transport (Ballantyne et al., 2013; Csank et al., 2011c; Ballantyne et al., 2010).

By analyzing differences in meridional heat transport across ocean and atmosphere components of the Earth System, the strength of the AMOC, and the heat flux between ocean and atmosphere in the North Atlantic to Arctic realm as a response to enhanced ocean vertical mixing, we show that the impact of a more vigorously stirred ocean on high latitude climate may strongly depend on the geography present in the model. From the viewpoint of ocean circulation, we see that the most relevant difference between the employed Pliocene and Miocene setups is the state of ocean gateways. While the Bering Strait is closed in both setups, a state that has been shown to increase meridional ocean heat transport in the Atlantic Ocean and warmth in the North Atlantic realm (Otto-Bliesner et al., 2017; Stepanek et al., 2020), a relevant difference in ocean gateways between both model setups is that of the CAS and of the Tethys. While enhanced ocean vertical mixing increases ocean heat transport towards the North in the Pliocene, the respective ocean heat transport increase in a geography configuration characteristic for the Miocene is rather towards the south. This can be explained by vertical mixing enhancing ocean heat transport in the preferred direction the climate state has previously been primed for. For the Pliocene this direction is more northward, for the Miocene it is rather southward (Fig. 12). State-dependency of the impact of enhanced ocean vertical mixing on the direction of meridional heat transport in the ocean can be understood in the larger context of the evolution of the interhemispheric partition of meridional heat transport directions across the Cenozoic. Gateway configuration was more favourable to southward ocean heat transport in the early Cenozoic with open Drake Passage and CAS. Over time, and together with gateway reconfiguration, meridional ocean heat transport oriented towards the north, with the modern state of gateways favouring a strong northward heat transport across all latitudes of the Atlantic Ocean basin (Bice et al., 2000). Assuming that the CAS was open during the Early Pliocene to an extent that allowed ocean heat transport to still be sufficiently impacted, our findings suggest that at that time enhanced ocean vertical mixing may have caused Arctic warmth via a more indirect atmospheric route rather than via the obvious pathway of enhanced northward ocean meridional heat transport.

There are other possible mechanisms that could provide similarly plausible explanations for a warmer Arctic, including different cloud and vegetation types in other background climates (Arima et al., 2026; Lohmann et al., 2022). Although near-surface warming may also arise from atmospheric processes related to clouds (Ceppi and Nowack, 2021), enhanced ocean vertical mixing has been shown to reduce discrepancies between reconstructed (Lear et al., 2015) and simulated deep-ocean temperatures, particularly for the Miocene (Lohmann et al., 2022). Because deep-ocean temperatures are closely linked to the efficiency of vertical heat exchange across the water column, one may infer that ocean mixing processes play a crucial role in explaining the vertical temperature structure in warm past climates. This motivates consideration of processes and model mechanisms that increase ocean vertical mixing in warm climates in future research.

5.3 Towards resolving ocean mixing processes: parameterization and future model development

We argue that ocean model processes that enhance the vertical distribution of heat in the water column and that reduce the dependence on parameterized vertical mixing constitute a promising direction for future paleoclimate research. Ocean vertical mixing parameterizations act as

https://doi.org/10.5194/egusphere-2026-4723
Preprint. Discussion started: 18 August 2026

surrogates for unresolved sub-grid scale vertical processes, including shear-driven turbulence, diapycnal mixing, convective adjustment, and boundary layer turbulence (Zhu et al., 2022). Separately, the effects of unresolved mesoscale eddies, which also indirectly influence diapycnal mixing via submesoscale processes and interal wave generation, are addressed through parameterizations such as that by Gent-McWilliams (Gent, 1995). While enhanced vertical mixing is employed here in a paleoclimatic context, its influence on high-latitude warming has also been demonstrated for the recent climate (Lohmann, 2020). To reproduce observed large-scale circulation patterns and water-mass properties, parameter values must be constrained by prior knowledge, theoretical considerations, or plausible ranges. If the dynamics of warm climates differ from those for which parameter values were originally defined, and if models fail to reproduce reconstructed conditions such as those of the Early Pliocene, the unmodified applicability of parameters derived from modern calibration must be questioned.

However, this is a common problem amongst climate models employed for paleoclimate research at tectonic timescales (Zhu et al., 2024), where the demand to spin up climate models to substantially different climate states, regularly including paleogeographic configurations very different from today, necessitates employing models at lower spatial resolution than commonly done for CMIP-style simulations of recent to near-future climates.

Several limitations of our study should be acknowledged. First, the Early Pliocene is bracketed by Pliocene and Miocene simulations rather than represented by a dedicated time-slice experiment. This could be remedied by more modelling groups running the dedicated Early Pliocene experiment of PlioMIP3 (Haywood et al., 2024). Second, proxy coverage of the Arctic Ocean remains spatially sparse, highlighting the necessity for better coverage for reconstructions of past Arctic environmental conditions across space and time. Third, enhanced vertical mixing is

https://doi.org/10.5194/egusphere-2026-4723
Preprint. Discussion started: 18 August 2026

implemented through a parameter perturbation intended to represent unresolved ocean processes rather than a direct reconstruction of Early Pliocene mixing rates (Wang et al., 2019; Chen et al., 2024; Song et al., 2022). Consequently, our conclusions concern the plausibility and dynamical consistency of a seasonally ice-free Arctic Ocean rather than a unique reconstruction of Early Pliocene climate conditions.

The development of models capable of dynamically representing mixing-related processes (e.g. eddies, wave-braking, different tidal dynamics in altered basin geometries) at a computational efficiency sufficient to equilibrate climate models when simulating past warm climates much different from today will therefore be central to advancing reconstructions of past warm Arctic climates and exploring the causes for model–proxy mismatches. This study underscores the value of combining boundary conditions and forcing experiments from intercomparison projects (e.g. PlioMIP, MioMIP) with parameter-adjustment analyses (Lohmann et al., 2022; Otto-Bliesner et al., 2017; Mikolajewicz et al., 2025; Ramos et al., 2022; Kapsch et al., 2022), which remains essential for constraining model behavior against geological evidence.

6. Conclusions

In conclusion, this study provides new insights into the Arctic climate during the Early Pliocene. We demonstrate that the Arctic Ocean was ice-free during summer under atmospheric CO_2 concentrations comparable to present-day levels if we consider the impact of more vigorous mixing in the ocean as plausible. However, our results also indicate that sea ice remained a persistent feature during winter, even under these warm climate conditions. The continued mismatch between Arctic proxy records and climate model simulations that are based solely on reconstructed geography and elevated CO_2 levels highlights the critical role of meridional heat transport, which in our simulations is amplified by enhanced vertical mixing. We explicitly hint to other unresolved processes contributing to shaping Arctic sea ice dynamics.

Both proxy evidence and model output here suggest that the Arctic climate system of the Early Pliocene operated under fundamentally different dynamics than today's Arctic, despite similar atmospheric CO_2 concentrations. These dynamics are not necessarily captured by climate models developed, tested, and calibrated for the modern climate system. This discrepancy may stem from unresolved physical processes in the models (e.g., enhanced vertical mixing by tides or other mechanisms) or inaccuracies in the representation of Arctic geography. Enhanced ocean mixing should therefore be viewed as one physically plausible mechanism capable of reducing model–proxy mismatch rather than as the unique explanation for Early Pliocene Arctic warmth.

Resolving these uncertainties is essential for accurately constraining future Arctic climate trajectories in a rapidly warming world. Our results demonstrate that the climatic impact of enhanced vertical ocean mixing depends strongly on gateway configuration. To assess the robustness of these heat transport pathways across models, future studies should extend this analysis using multi-model ensembles. In addition, paleoclimate simulations with climate models that rely less on vertical mixing to parameterize unresolved ocean processes would help disentangle the mechanisms driving past warm Arctic climates. Our findings provide a strong rationale for further investigation within the PlioMIP3 Early Pliocene multi-model ensemble (Haywood et al., 2024).

Code and data availability

Software employed in the context of creating simulations, analyses, and plots for the purpose of the study contains the following elements:

1. **COSMOS suite of Earth System Models**

https://doi.org/10.5194/egusphere-2026-4723
Preprint. Discussion started: 18 August 2026

a) **software**

COSMOS has been formerly developed by the Max Planck Institute for Meteorology in Hamburg/Germany (MPI-Met; https://mpimet.mpg.de/en). We have access to this software package, that includes model source code and accompanying scripts to compile, set up and run the model, via an agreement with the MPI-Met. The model is not publicly available. Copies of the software must be requested and obtained directly from the MPI-Met. Distribution of the software is subject to a license agreement.

b) **COSMOS climate model output**

The climate model output created by us and employed in the context of this study is available upon request. Some of the variables analyzed here have already been made available to the community via

i. the PlioMIP2 model output server (access available upon request by Julia Tindall, School of Earth and Environment, University of Leeds)
ii. a data publication (https://doi.pangaea.de/10.1594/PANGAEA.927137) linked to the publication by Lohmann et al. (2022) available at https://agupubs.onlinelibrary.wiley.com/doi/full/10.1029/2020PA003953

2. **Climate Data Operators**

Analysis of the output of the software has been largely performed based on Climate Data Operators (CDO) that are available to the public via https://code.mpimet.mpg.de/projects/cdo or software distribution channels

3. **Python-scripts**

We have created various scripts to analyze the output of the software and to produce the various plots employing publicly available python packages.

Some analyses in the python scripts process model data via calls to the CDO. These python scripts are made available upon request. Towards creating a model-intercomparison of

https://doi.org/10.5194/egusphere-2026-4723
Preprint. Discussion started: 18 August 2026

COSMOS with other common climate models, scripts that derive Figures 4-7 do not only process and visualize COSMOS model output but also refer to corresponding climate model output of the *piControl* simulation of various CMIP3/CMIP5/CMIP6 models. Any CMIP model output used by these scripts is generally available to the public and has been obtained from the Earth System Grid Federation. The search catalog is available at https://esgf-metagrid.cloud.dkrz.de/search. Simulations employed are referenced in the manuscript, a more detailed overview is available from the supplement to the manuscript by Khoo et al. (2025) available at https://cp.copernicus.org/articles/21/299/2025/cp-21-299-2025-supplement.pdf, in particular their Table S4.

Author Contributions:

J.K.: Writing – original draft, Conceptualization, Writing – review & editing, Methodology, Resources, Funding acquisition, Visualization. **C.S.:** Writing – original draft, Conceptualization, Writing – review & editing, Data curation, Validation, Formal analysis, Software, Visualization. **S.T.B**.: Writing – original draft, Investigation, Writing – review & editing, Methodology**. S.D.S**.: Writing – original draft, Investigation, Writing – review & editing, Funding acquisition. **G.L**.: Writing – original draft, Conceptualization, Investigation, Writing – review & editing, Methodology, Resources, Funding acquisition.

Competing Interest

Authors declare that they have no competing interests.

https://doi.org/10.5194/egusphere-2026-4723
Preprint. Discussion started: 18 August 2026

Acknowledgments

This research used samples and data provided by the International Ocean Discovery Program/Ocean Drilling Program (IODP/ODP). We sincerely thank the staff at the IODP core repository in Bremen, Germany, for all their help during various sampling parties. JK, C.S., S.d.S, and G.L. are funded by the European Union through the ERC grant # 101118519. Claude Sonnet 5 (Anthropic) and ChatGPT were used to assist with language editing and to help identify structural and narrative-clarity issues in earlier drafts; all resulting text revisions were written and finalized by the authors. Some of the Python and Shell scripts used to post-process data and visualize model output were developed and debugged with the assistance of Claude Sonnet 5 (Anthropic), including the identification and correction of coding errors affecting figure layout. All model-derived content displayed in figures represents unaltered model output, and the authors reviewed and verified all figures and take full responsibility for their content.

References

Allende, S., Treguier, A. M., Lique, C., de Boyer Montégut, C., Massonnet, F., Fichefet, T., and Barthélemy, A.: Impact of ocean vertical-mixing parameterization on Arctic sea ice and upper-ocean properties using the NEMO-SI3 model, Geoscientific Model Development, 17, 7445-7466, 2024.

Arima, N., Yoshimori, M., Abe-Ouchi, A., O'ishi, R., Chan, W.-L., Sherriff-Tadano, S., and Ogura, T.: Impact of the temperature-cloud phase relationship on the simulated Arctic warming during the Last Interglacial, Climate of the Past, 22, 891-913, 2026.

Bachem, P. E., Risebrobakken, B., De Schepper, S., and McClymont, E. L.: Highly variable Pliocene sea surface conditions in the Norwegian Sea, Climate of the Past, 13, 1153-1168, 2017.

Ballantyne, A. P., Axford, Y., Miller, G. H., Otto-Bliesner, B. L., Rosenbloom, N., and White, J. W. C.: The amplification of Arctic terrestrial surface temperatures by reduced sea-ice extent during the Pliocene, Palaeogeography, Palaeoclimatology, Palaeoecology, 386, 59-67, https://doi.org/10.1016/j.palaeo.2013.05.002, 2013.

Ballantyne, A. P., Greenwood, D., Sinninghe Damsté, J., Csank, A., Eberle, J., and Rybczynski, N.: Significantly warmer Arctic surface temperatures during the Pliocene indicated by multiple independent proxies, Geology, 38, 603-606, 2010.

Belt, S. T., Brown, T. A., Ringrose, A. E., Cabedo-Sanz, P., Mundy, C. J., Gosselin, M., and Poulin, M.: Quantitative measurement of the sea ice diatom biomarker IP25 and sterols in Arctic sea ice and underlying sediments: Further considerations for palaeo sea ice reconstruction, Organic Geochemistry, 62, 33-45, 2013.

Berends, C. J., de Boer, B., Dolan, A. M., Hill, D. J., and van de Wal, R. S. W.: Modelling ice sheet evolution and atmospheric CO2 during the Late Pliocene, Climate of the Past, 15, 1603-1619, 10.5194/cp-15-1603-2019, 2019.

Bice, K. L., Scotese, C. R., Seidov, D., and Barron, E. J.: Quantifying the role of geographic change in Cenozoic ocean heat transport using uncoupled atmosphere and ocean models, Palaeogeography, Palaeoclimatology, Palaeoecology, 161, 295-310, 2000.

Bjerknes, J.: Atlantic air-sea interaction, in: Advances in geophysics, Elsevier, 1-82, 1964.

Brigham-Grette, J. and Carter, L.: Pliocene marine transgressions of northern Alaska: circumarctic correlations and paleoclimatic interpretations, Arctic, 74-89, 1992.

Brigham-Grette, J., Melles, M., Minyuk, P., Andreev, A., Tarasov, P., DeConto, R., Koenig, S., Nowaczyk, N., Wennrich, V., and Rosén, P.: Pliocene warmth, polar amplification, and stepped Pleistocene cooling recorded in NE Arctic Russia, Science, 340, 1421-1427, 2013.

Brovkin, V., Raddatz, T., Reick, C. H., Claussen, M., and Gayler, V.: Global biogeophysical interactions between forest and climate, Geophysical research letters, 36, 2009.

https://doi.org/10.5194/egusphere-2026-4723
Preprint. Discussion started: 18 August 2026

Brown, T. A., Belt, S. T., Tatarek, A., and Mundy, C.: Source identification of the Arctic sea ice proxy IP25, Nature Communications, 5, 4197, 2014.

Burke, K. D., Williams, J. W., Chandler, M. A., Haywood, A. M., Lunt, D. J., and Otto-Bliesner, B. L.: Pliocene and Eocene provide best analogs for near-future climates, Proceedings of the National Academy of Sciences, 115, 13288-13293, 2018.

Burls, N. J., Bradshaw, C., De Boer, A. M., Herold, N., Huber, M., Pound, M., Donnadieu, Y., Farnsworth, A., Frigola, A., and Gasson, E.: Simulating miocene warmth: insights from an opportunistic multi-model ensemble (MioMIP1), Paleoceanography and Paleoclimatology, 36, e2020PA004054, 2021a.

Burls, N. J., Bradshaw, C. D., De Boer, A. M., Herold, N., Huber, M., Pound, M., Donnadieu, Y., Farnsworth, A., Frigola, A., Gasson, E., von der Heydt, A. S., Hutchinson, D. K., Knorr, G., Lawrence, K. T., Lear, C. H., Li, X., Lohmann, G., Lunt, D. J., Marzocchi, A., Prange, M., Riihimaki, C. A., Sarr, A.-C., Siler, N., and Zhang, Z.: Simulating Miocene Warmth: Insights From an Opportunistic Multi-Model Ensemble (MioMIP1), Paleoceanography and Paleoclimatology, 36, e2020PA004054, https://doi.org/10.1029/2020PA004054, 2021b.

Chen, Y., Song, P., Chen, X., and Lohmann, G.: Glacial AMOC shoaling despite vigorous tidal dissipation: Vertical stratification matters, Climate of the Past, 20, 2001-2015, 2024.

Clotten, C., Stein, R., Fahl, K., Schreck, M., Risebrobakken, B., and De Schepper, S.: On the causes of Arctic sea ice in the warm Early Pliocene, Scientific reports, 9, 989, 2019.

Cronin, T. M., Whatley, R., Wood, A., Tsukagoshi, A., Ikeya, N., Brouwers, E. M., and Briggs Jr, W.: Microfaunal evidence for elevated Pliocene temperatures in the Arctic Ocean, Paleoceanography, 8, 161-173, 1993.

Csank, A., Patterson, W., Eglington, B., Rybczynski, N., and Basinger, J.: Climate variability in the Early Pliocene Arctic: Annually resolved evidence from stable isotope values of sub-fossil wood, Ellesmere Island, Canada, Palaeogeography, Palaeoclimatology, Palaeoecology, 308, 339-349, 2011a.

Csank, A. Z., Tripati, A. K., Patterson, W. P., Eagle, R. A., Rybczynski, N., Ballantyne, A. P., and Eiler, J. M.: Estimates of Arctic land surface temperatures during the early Pliocene from two novel proxies, Earth and Planetary Science Letters, 304, 291-299, 2011b.

Csank, A. Z., Tripati, A. K., Patterson, W. P., Eagle, R. A., Rybczynski, N., Ballantyne, A. P., and Eiler, J. M.: Estimates of Arctic land surface temperatures during the early Pliocene from two novel proxies, Earth and Planetary Science Letters, 304, 291-299, https://doi.org/10.1016/j.epsl.2011.02.030, 2011c.

de Nooijer, W., Zhang, Q., Li, Q., Zhang, Q., Li, X., Zhang, Z., Guo, C., Nisancioglu, K. H., Haywood, A. M., and Tindall, J. C.: Evaluation of Arctic warming in mid-Pliocene climate simulations, Climate of the Past, 16, 2325-2341, 2020.

https://doi.org/10.5194/egusphere-2026-4723
Preprint. Discussion started: 18 August 2026

De Schepper, S. and McClymont, E. L.: Transition from late Neogene to early Pleistocene environments, in: Encyclopedia of Quaternary Science (Third edition), edited by: Elias, S., Elsevier, Oxford, 611-628, https://doi.org/10.1016/B978-0-323-99931-1.00121-5, 2025.

De Schepper, S., Gibbard, P. L., Salzmann, U., and Ehlers, J.: A global synthesis of the marine and terrestrial evidence for glaciation during the Pliocene Epoch, Earth-Science Reviews, 135, 83-102, 2014.

Docquier, D., Grist, J. P., Roberts, M. J., Roberts, C. D., Semmler, T., Ponsoni, L., Massonnet, F., Sidorenko, D., Sein, D. V., and Iovino, D.: Impact of model resolution on Arctic sea ice and North Atlantic Ocean heat transport, 2019.

Dowsett, H., Dolan, A., Rowley, D., Moucha, R., Forte, A. M., Mitrovica, J. X., Pound, M., Salzmann, U., Robinson, M., and Chandler, M.: The PRISM4 (mid-Piacenzian) paleoenvironmental reconstruction, Climate of the Past, 12, 1519-1538, 2016.

Dowsett, H. J., Foley, K. M., Stoll, D. K., Chandler, M. A., Sohl, L. E., Bentsen, M., Otto-Bliesner, B. L., Bragg, F. J., Chan, W.-L., and Contoux, C.: Sea surface temperature of the mid-Piacenzian ocean: a data-model comparison, Scientific reports, 3, 2013, 2013.

Fedorov, A. V., Brierley, C., Lawrence, K. T., Liu, Z., Dekens, P., and Ravelo, A.: Patterns and mechanisms of early Pliocene warmth, Nature, 496, 43-49, 2013.

Gent, P. R., Willebrand, J., McDougall, T. J., and McWilliams, J. C.: Parameterizing eddy-induced tracer transports in ocean circulation models, Journal of physical oceanography, 25, 463-474, 1995.

Gladenkov, A. Y., Oleinik, A. E., Marincovich Jr, L., and Barinov, K. B.: A refined age for the earliest opening of Bering Strait, Palaeogeography, Palaeoclimatology, Palaeoecology, 183, 321-328, 2002.

Hagemann, S. and Dümenil, L.: A parametrization of the lateral waterflow for the global scale, Climate dynamics, 14, 17-31, 1997.

Hagemann, S. and Gates, L. D.: Validation of the hydrological cycle of ECMWF and NCEP reanalyses using the MPI hydrological discharge model, Journal of Geophysical Research: Atmospheres, 106, 1503-1510, 2001.

Hall, J. R., Allison, M. S., Papadopoulos, M. T., Barfod, D. N., and Jones, S. M.: Timing and consequences of Bering Strait opening: New insights from 40Ar/39Ar dating of the Barmur Group (Tjörnes beds), northern Iceland, Paleoceanography and Paleoclimatology, 38, e2022PA004539, 2023.

Haywood, A. M., Dowsett, H. J., Dolan, A. M., Rowley, D., Abe-Ouchi, A., Otto-Bliesner, B., Chandler, M. A., Hunter, S. J., Lunt, D. J., and Pound, M.: The Pliocene model intercomparison project (PlioMIP) phase 2: scientific objectives and experimental design, Climate of the Past, 12, 663-675, 2016.

https://doi.org/10.5194/egusphere-2026-4723
Preprint. Discussion started: 18 August 2026

Haywood, A. M., Hill, D., Dolan, A., Otto-Bliesner, B. L., Bragg, F., Chan, W.-L., Chandler, M. A., Contoux, C., Dowsett, H. J., and Jost, A.: Large-scale features of Pliocene climate: results from the Pliocene Model Intercomparison Project, Climate of the Past, 9, 191-209, 2013.

Haywood, A. M., Tindall, J. C., Burton, L., Chandler, M., Dolan, A. M., Dowsett, H. J., Feng, R., Fletcher, T., Foley, K. M., and Hill, D.: Pliocene Model Intercomparison Project Phase 3 (PlioMIP3)–Science Plan and Experimental Design, Global and Planetary Change, 232, 104316, 2024.

Haywood, A. M., Tindall, J. C., Dowsett, H. J., Dolan, A. M., Foley, K. M., Hunter, S. J., Hill, D. J., Chan, W.-L., Abe-Ouchi, A., and Stepanek, C.: The Pliocene Model Intercomparison Project Phase 2: large-scale climate features and climate sensitivity, Climate of the Past, 16, 2095-2123, 2020.

Herbert, T. D., Lawrence, K. T., Tzanova, A., Peterson, L. C., Caballero-Gill, R., and Kelly, C. S.: Late Miocene global cooling and the rise of modern ecosystems, Nature Geoscience, 9, 843-847, 2016.

Herold, N., Huber, M., Müller, R. D., and Seton, M.: Modeling the Miocene climatic optimum: Ocean circulation, Paleoceanography, 27, https://doi.org/10.1029/2010PA002041, 2012.

Herold, N., Seton, M., Müller, R., You, Y., and Huber, M.: Middle Miocene tectonic boundary conditions for use in climate models, Geochemistry, Geophysics, Geosystems, 9, 2008.

Hossain, A., Knorr, G., Jokat, W., and Lohmann, G.: Opening of the Fram Strait led to the establishment of a modern-like three-layer stratification in the Arctic Ocean during the Miocene, arktos, 7, 1-12, 2021.

Hossain, A., Knorr, G., Lohmann, G., Stärz, M., and Jokat, W.: Simulated thermohaline fingerprints in response to different Greenland-Scotland Ridge and Fram Strait subsidence histories, Paleoceanography and Paleoclimatology, 35, e2019PA003842, 2020.

Howell, F. W., Haywood, A. M., Otto-Bliesner, B. L., Bragg, F., Chan, W.-L., Chandler, M. A., Contoux, C., Kamae, Y., Abe-Ouchi, A., and Rosenbloom, N. A.: Arctic sea ice simulation in the PlioMIP ensemble, Climate of the Past, 12, 749-767, 2016.

Intrieri, J., Fairall, C., Shupe, M., Persson, P., Andreas, E., Guest, P., and Moritz, R.: An annual cycle of Arctic surface cloud forcing at SHEBA, Journal of Geophysical Research: Oceans, 107, SHE 13-11-SHE 13-14, 2002.

Jahn, A., Holland, M. M., and Kay, J. E.: Projections of an ice-free Arctic Ocean, Nature Reviews Earth & Environment, 5, 164-176, 2024.

Jansen, E., Fronval, T., Rack, F., and Channell, J. E.: Pliocene-Pleistocene ice rafting history and cyclicity in the Nordic Seas during the last 3.5 Myr, Paleoceanography, 15, 709-721, 2000.

Jungclaus, J. H., Keenlyside, N., Botzet, M., Haak, H., Luo, J.-J., Latif, M., Marotzke, J., Mikolajewicz, U., and Roeckner, E.: Ocean circulation and tropical variability in the coupled model ECHAM5/MPI-OM, Journal of climate, 19, 3952-3972, 2006.

https://doi.org/10.5194/egusphere-2026-4723
Preprint. Discussion started: 18 August 2026

Kim, Y.-H., Min, S.-K., Gillett, N. P., Notz, D., and Malinina, E.: Observationally-constrained projections of an ice-free Arctic even under a low emission scenario, Nature Communications, 14, 3139, 2023.

Kinnard, C., Zdanowicz, C. M., Fisher, D. A., Isaksson, E., de Vernal, A., and Thompson, L. G.: Reconstructed changes in Arctic sea ice over the past 1,450 years, Nature, 479, 509-U231, 10.1038/nature10581, 2011.

Kleiven, H. F., Jansen, E., Fronval, T., and Smith, T.: Intensification of Northern Hemisphere glaciations in the circum Atlantic region (3.5–2.4 Ma)–ice-rafted detritus evidence, Palaeogeography, Palaeoclimatology, Palaeoecology, 184, 213-223, 2002.

Knies, J., Cabedo-Sanz, P., Belt, S. T., Baranwal, S., Fietz, S., and Rosell-Melé, A.: The emergence of modern sea ice cover in the Arctic Ocean, Nature communications, 5, 5608, 2014a.

Knies, J., Mattingsdal, R., Fabian, K., Grosfjeld, K., Baranwal, S., Husum, K., De Schepper, S., Vogt, C., Andersen, N., Matthiessen, J., Andreassen, K., Jokat, W., Nam, S.-I., and Gaina, C.: Effect of early Pliocene uplift on late Pliocene cooling in the Arctic-Atlantic gateway, Earth and Planetary Science Letters, 387, 132-144, 10.1016/j.epsl.2013.11.007, 2014b.

Lisiecki, L. E. and Raymo, M. E.: A Pliocene-Pleistocene stack of 57 globally distributed benthic δ18O records, Paleoceanography, 20, 2005.

Lohmann, G., Knorr, G., Hossain, A., and Stepanek, C.: Effects of CO2 and ocean mixing on Miocene and Pliocene temperature gradients, Paleoceanography and Paleoclimatology, 37, e2020PA003953, 2022.

Lunt, D. J., Foster, G. L., Haywood, A. M., and Stone, E. J.: Late Pliocene Greenland glaciation controlled by a decline in atmospheric CO2 levels, Nature, 454, 1102-1105, 2008.

Marincovich Jr, L.: Central American paleogeography controlled Pliocene Arctic Ocean molluscan migrations, Geology, 28, 551-554, 2000.

Marsland, S. J., Haak, H., Jungclaus, J. H., Latif, M., and Röske, F.: The Max-Planck-Institute global ocean/sea ice model with orthogonal curvilinear coordinates, Ocean modelling, 5, 91-127, 2003.

Martínez-Botí, M. A., Foster, G. L., Chalk, T. B., Rohling, E. J., Sexton, P. F., Lunt, D. J., Pancost, R. D., Badger, M. P., and Schmidt, D. N.: Plio-Pleistocene climate sensitivity evaluated using high-resolution CO2 records, Nature, 518, 49-54, 2015.

Matthiessen, J., Knies, J., Vogt, C., and Stein, R.: Pliocene palaeoceanography of the Arctic Ocean and subarctic seas, Philosophical Transactions of the Royal Society A: Mathematical, Physical and Engineering Sciences, 367, 21-48, 2009.

McClymont, E. L., Ho, S. L., Ford, H. L., Bailey, I., Berke, M. A., Bolton, C. T., De Schepper, S., Grant, G. R., Groeneveld, J., Inglis, G. N., Karas, C., Patterson, M. O., Swann, G. E. A., Thirumalai, K., White, S. M., Alonso-Garcia, M., Anand, P., Hoogakker, B. A. A., Littler, K., Petrick, B. F., Risebrobakken, B., Abell, J. T., Crocker, A. J., de Graaf, F., Feakins, S. J., Hargreaves, J. C., Jones,

https://doi.org/10.5194/egusphere-2026-4723
Preprint. Discussion started: 18 August 2026

C. L., Markowska, M., Ratnayake, A. S., Stepanek, C., and Tangunan, D.: Climate Evolution Through the Onset and Intensification of Northern Hemisphere Glaciation, Reviews of Geophysics, 61, e2022RG000793, https://doi.org/10.1029/2022RG000793, 2023.

Miller, K. G., MouNtaiN, G. S., WriGht, J. D., and BroWNiNG, J. V.: A 180-million-year record of sea level and ice volume variations from continental margin and deep-sea isotopic records, Oceanography, 24, 40-53, 2011.

Moran, K., Backman, J., Brinkhuis, H., Clemens, S. C., Cronin, T., Dickens, G. R., Eynaud, F., Gattacceca, J., Jakobsson, M., Jordan, R. W., Kaminski, M., King, J., Koc, N., Krylov, A., Martinez, N., Matthiessen, J., McInroy, D., Moore, T. C., Onodera, J., O'Regan, M., Palike, H., Rea, B., Rio, D., Sakamoto, T., Smith, D. C., Stein, R., St John, K., Suto, I., Suzuki, N., Takahashi, K., Watanabe, M., Yamamoto, M., Farrell, J., Frank, M., Kubik, P., Jokat, W., and Kristoffersen, Y.: The Cenozoic palaeoenvironment of the Arctic Ocean, Nature, 441, 601-605, 10.1038/nature04800, 2006.

Notz, D. and Stroeve, J.: Observed Arctic sea-ice loss directly follows anthropogenic CO2 emission, Science, 354, 747-750, 10.1126/science.aag2345, 2016.

Oldeman, A. M., Baatsen, M. L., von der Heydt, A. S., van Delden, A. J., and Dijkstra, H. A.: Mid-Pliocene not analogous to high-CO 2 climate when considering Northern Hemisphere winter variability, Weather and Climate Dynamics, 5, 395-417, 2024.

Pacanowski, R. and Philander, S.: Parameterization of vertical mixing in numerical models of tropical oceans, J. phys. Oceanogr, 11, 1443-1451, 1981.

Patton, H., Alexandropoulou, N., Lasabuda, A. P., Knies, J., Andreassen, K., Winsborrow, M., Laberg, J. S., and Hubbard, A.: Glacial erosion and Quaternary landscape development of the Eurasian Arctic, Earth-Science Reviews, 104936, 2024.

Pieńkowski, A. J., Husum, K., Belt, S. T., Ninnemann, U., Köseoğlu, D., Divine, D. V., Smik, L., Knies, J., Hogan, K., and Noormets, R.: Seasonal sea ice persisted through the Holocene Thermal Maximum at 80 N, Communications Earth & Environment, 2, 124, 2021.

Pörtner, H.-O., Roberts, D. C., Masson-Delmotte, V., Zhai, P., Tignor, M., Poloczanska, E., and Weyer, N.: The ocean and cryosphere in a changing climate, IPCC special report on the ocean and cryosphere in a changing climate, 1155, 10.1017, 2019.

Raddatz, T. J., Reick, C., Knorr, W., Kattge, J., Roeckner, E., Schnur, R., Schnitzler, K.-G., Wetzel, P., and Jungclaus, J.: Will the tropical land biosphere dominate the climate–carbon cycle feedback during the twenty-first century?, Climate dynamics, 29, 565-574, 2007.

Rahaman, W., Smik, L., Köseoğlu, D., Lathika, N., Tarique, M., Thamban, M., Haywood, A., Belt, S. T., and Knies, J.: Reduced Arctic sea ice extent during the mid-Pliocene Warm Period concurrent with increased Atlantic-climate regime, Earth and Planetary Science Letters, 550, 116535, 2020.

Redi, M. H.: Oceanic isopycnal mixing by coordinate rotation, Journal of Physical Oceanography, 12, 1154-1158, 1982.

https://doi.org/10.5194/egusphere-2026-4723
Preprint. Discussion started: 18 August 2026

Reinink-Smith, L. M. and Leopold, E. B.: Warm climate in the late Miocene of the south coast of Alaska and the occurrence of Podocarpaceae pollen, Palynology, 29, 205-262, 10.1080/01916122.2005.9989607, 2005.

Robinson, M. M.: New quantitative evidence of extreme warmth in the Pliocene Arctic, Stratigraphy, 6, 265, 2009.

Rybczynski, N., Gosse, J. C., Richard Harington, C., Wogelius, R. A., Hidy, A. J., and Buckley, M.: Mid-Pliocene warm-period deposits in the High Arctic yield insight into camel evolution, Nature communications, 4, 1550, 2013.

Salzmann, U., Williams, M., Haywood, A. M., Johnson, A. L. A., Kender, S., and Zalasiewicz, J.: Climate and environment of a Pliocene warm world, Palaeogeography, Palaeoclimatology, Palaeoecology, 309, 1-8, https://doi.org/10.1016/j.palaeo.2011.05.044, 2011.

Salzmann, U., Dolan, A. M., Haywood, A. M., Chan, W.-L., Voss, J., Hill, D. J., Abe-Ouchi, A., Otto-Bliesner, B., Bragg, F. J., and Chandler, M. A.: Challenges in quantifying Pliocene terrestrial warming revealed by data–model discord, Nature Climate Change, 3, 969-974, 2013.

Schulzweida, U.: CDO User Guide (2.3.0), Zenodo [code], https://doi.org/10.5281/zenodo.10020800, 2023.

Selivanova, J., Iovino, D., and Cocetta, F.: Past and future of the Arctic sea ice in High-Resolution Model Intercomparison Project (HighResMIP) climate models, The Cryosphere, 18, 2739-2763, 2024.

Slater, T., Lawrence, I. R., Otosaka, I. N., Shepherd, A., Gourmelen, N., Jakob, L., Tepes, P., Gilbert, L., and Nienow, P.: Review article: Earth's ice imbalance, The Cryosphere, 15, 233-246, 10.5194/tc-15-233-2021, 2021.

Smik, L., Cabedo-Sanz, P., and Belt, S. T.: Semi-quantitative estimates of paleo Arctic sea ice concentration based on source-specific highly branched isoprenoid alkenes: A further development of the PIP25 index, Organic Geochemistry, 92, 63-69, 2016.

Song, P., Sidorenko, D., Scholz, P., Thomas, M., and Lohmann, G.: The tidal effects in the Finite-volumE Sea ice–Ocean Model (FESOM2. 1): a comparison between parameterised tidal mixing and explicit tidal forcing, Geoscientific Model Development Discussions, 2022, 1-42, 2022.

Sosdian, S. M., Greenop, R., Hain, M., Foster, G. L., Pearson, P. N., and Lear, C. H.: Constraining the evolution of Neogene ocean carbonate chemistry using the boron isotope pH proxy, Earth and Planetary Science Letters, 498, 362-376, 2018.

Stap, L. B., de Boer, B., Ziegler, M., Bintanja, R., Lourens, L. J., and van de Wal, R. S.: CO2 over the past 5 million years: Continuous simulation and new δ11B-based proxy data, Earth and Planetary Science Letters, 439, 1-10, 2016.

https://doi.org/10.5194/egusphere-2026-4723
Preprint. Discussion started: 18 August 2026

Stärz, M., Jokat, W., Knorr, G., and Lohmann, G.: Threshold in North Atlantic-Arctic Ocean circulation controlled by the subsidence of the Greenland-Scotland Ridge, Nature communications, 8, 15681, 2017.

Stein, R.: The Late Mesozoic-Cenozoic Arctic Ocean Climate and Sea Ice History: A Challenge for Past and Future Scientific Ocean Drilling, Paleoceanography and Paleoclimatology, 34, 1851-1894, 10.1029/2018pa003433, 2019.

Stein, R., Fahl, K., Schreck, M., Knorr, G., Niessen, F., Forwick, M., Gebhardt, C., Jensen, L., Kaminski, M., Kopf, A., Matthiessen, J., Jokat, W., and Lohmann, G.: Evidence for ice-free summers in the late Miocene central Arctic Ocean, Nature Communications, 7, 11148, 10.1038/ncomms11148, 2016.

Steinthorsdottir, M., Coxall, H. K., de Boer, A. M., Huber, M., Barbolini, N., Bradshaw, C. D., Burls, N. J., Feakins, S. J., Gasson, E., Henderiks, J., Holbourn, A., Kiel, S., Kohn, M. J., Knorr, G., Kürschner, W. M., Lear, C. H., Liebrand, D., Lunt, D. J., Mörs, T., Pearson, P. N., Pound, M. J., Stoll, H., and Strömberg, C. A. E.: The Miocene: the Future of the Past, Paleoceanography and Paleoclimatology, n/a, e2020PA004037, https://doi.org/10.1029/2020PA004037, 2021.

Stepanek, C. and Lohmann, G.: Modelling mid-Pliocene climate with COSMOS, Geoscientific Model Development, 5, 1221-1243, 2012.

Stepanek, C., Samakinwa, E., Knorr, G., and Lohmann, G.: Contribution of the coupled atmosphere–ocean–sea ice–vegetation model COSMOS to the PlioMIP2, Climate of the Past, 16, 2275-2323, 2020.

Super, J. R., Thomas, E., Pagani, M., Huber, M., O'Brien, C., and Hull, P. M.: North Atlantic temperature and pCO2 coupling in the early-middle Miocene, Geology, 46, 519-522, 10.1130/g40228.1, 2018.

Tedford, R. H. and Harington, C. R.: An Arctic mammal fauna from the Early Pliocene of North America, Nature, 425, 388-390, 10.1038/nature01892, 2003.

Trenberth, K. E. and Caron, J. M.: Estimates of meridional atmosphere and ocean heat transports, Journal of Climate, 14, 3433-3443, 2001.

Wang, S., Wang, Q., Shu, Q., Scholz, P., Lohmann, G., and Qiao, F.: Improving the upper-ocean temperature in an ocean climate model (FESOM 1.4): Shortwave penetration versus mixing induced by nonbreaking surface waves, Journal of Advances in Modeling Earth Systems, 11, 545-557, 2019.

Zhang, J. and Steele, M.: Effect of vertical mixing on the Atlantic Water layer circulation in the Arctic Ocean, Journal of geophysical research: Oceans, 112, 2007.

Zhang, Q., Liu, B., Li, S., and Zhou, T.: Understanding models' global sea surface temperature bias in mean state: From CMIP5 to CMIP6, Geophysical Research Letters, 50, e2022GL100888, 2023.

https://doi.org/10.5194/egusphere-2026-4723
Preprint. Discussion started: 18 August 2026

Zhang, Y. G., Pagani, M., Liu, Z., Bohaty, S. M., and DeConto, R.: A 40-million-year history of atmospheric CO2, Philosophical Transactions of the Royal Society A: Mathematical, Physical and Engineering Sciences, 371, 20130096, 2013.

Zhu, J., Poulsen, C. J., and Otto-Bliesner, B. L.: Modeling past hothouse climates as a means for assessing Earth system models and improving the understanding of warm climates, Annual Review of Earth and Planetary Sciences, 52, 351-378, 2024.

Zhu, Y., Zhang, R.-H., Moum, J. N., Wang, F., Li, X., and Li, D.: Physics-informed deep-learning parameterization of ocean vertical mixing improves climate simulations, National Science Review, 9, nwac044, 2022.